

**SYNTHESES AND BIOLOGICAL APPLICATIONS OF SELECTED N-CONTAINING  
HETEROCYCLES: RECENT ADVANCES OF DERIVATIVES OF AZIRIDINES,  
TRIAZOLES, AND PIPERAZINES**

DOI: <http://dx.medra.org/10.17374/targets.2025.28.280>

**Serena Vittorio,<sup>a</sup> Christian Dank,<sup>b</sup> Laura Ielo<sup>c,d\*</sup>**

<sup>a</sup>*Dipartimento di Scienze Farmaceutiche, Università degli Studi di Milano, Milano, Italy*

<sup>b</sup>*Institute of Organic Chemistry, University of Vienna, Vienna, Austria*

<sup>c</sup>*Department of Chemistry, University of Turin, Turin, Italy*

<sup>d</sup>*Institute of Applied Synthetic Chemistry, TU Wien, Vienna, Austria*  
(e-mail: [laura.ielo@unito.it](mailto:laura.ielo@unito.it))

**Abstract.** *Heterocycles are organic cyclic compounds characterized by one or more heteroatoms in their structures. The most diffuse examples in chemistry are the five- or six-membered heterocycles bearing a nitrogen, oxygen, and/or sulfur atoms. They are the largest and most varied family of organic compounds showing several biological activities and represent more than 50% of the nowadays existing drugs. In this chapter, the syntheses and biological applications of aziridine, triazole, and piperazine derivatives are reported, considering their importance in organic chemistry and medicinal chemistry.*

## Contents

1. Introduction
2. Aziridines
  - 2.1. Syntheses of aziridines from alkenes
  - 2.2. Syntheses of aziridines from imines
  - 2.3. Miscellaneous
  - 2.4. Biological activities of aziridines
    - 2.4.1. Activities of aziridines against oncological targets
    - 2.4.2. Different biological targets of aziridines
3. Triazoles
  - 3.1. Synthesis of 1,2,3-triazoles
    - 3.1.1. Synthesis of 1,2,3-triazoles from azides
    - 3.1.2. Synthesis of 1,2,3-triazoles: azide-free approaches
  - 3.2. Synthesis of 1,2,4-triazoles
    - 3.2.2. Synthesis of 1,2,4-triazoles from hydrazones
    - 3.2.3. Miscellaneous
  - 3.3. Biological applications of triazoles
4. Piperazines
  - 4.1. Syntheses of piperazines *via* ketopiperazine reduction and *N*-alkylation
  - 4.2. Syntheses of piperazines *via* catalysis
  - 4.3. Miscellaneous
  - 4.4. Biological activities of piperazine derivatives
5. Conclusion
- Acknowledgements
- References

## 1. Introduction

Heterocycles are organic cyclic compounds characterized by at least one heteroatom in their structure. The presence of heteroatoms confers them physical and chemical properties that are quite distinct from those of their all-carbon-ring analogs.<sup>1</sup> The smallest existing heterocycles are 3-membered rings possessing different heteroatoms, such as nitrogen, oxygen, and sulfur leading to aziridines,<sup>2</sup> epoxides,<sup>3</sup> and thiiranes,<sup>4</sup> respectively. The group of heterocycles with widest abundance are five- or six-membered rings bearing at least one nitrogen, oxygen, or sulfur atoms (*e.g.* furan,<sup>5</sup> thiophene,<sup>6</sup> pyrrole,<sup>7</sup> pyrazole,<sup>8</sup> imidazoles,<sup>9</sup> isoxazole,<sup>10</sup> pyridine<sup>11</sup>). Furthermore, fused rings are widely used in organic chemistry (*e.g.* indazoles,<sup>12</sup> benzopyrans,<sup>13</sup> benzofurans,<sup>14</sup>

purines<sup>15</sup>). Although less common, heterocycles are also found to possess heteroatoms other than nitrogen, oxygen, and sulfur (*e.g.* selenium, phosphorus).<sup>16</sup>

Heterocycles constitute the largest and most varied family of organic compounds showing several biological activities. More than 50% of the nowadays existing drugs possess in their structure at least one heterocyclic ring.<sup>17</sup> Among the huge variety of heterocyclic compounds, we decided to focus the attention on aziridines,<sup>18</sup> triazoles,<sup>19</sup> and piperazines<sup>20,21</sup> due to their importance in organic chemistry and medicinal chemistry (Figure 1). Thus, in this chapter, the recent advances in the syntheses and biological applications of aziridines, triazoles, and piperazines derivatives are discussed.

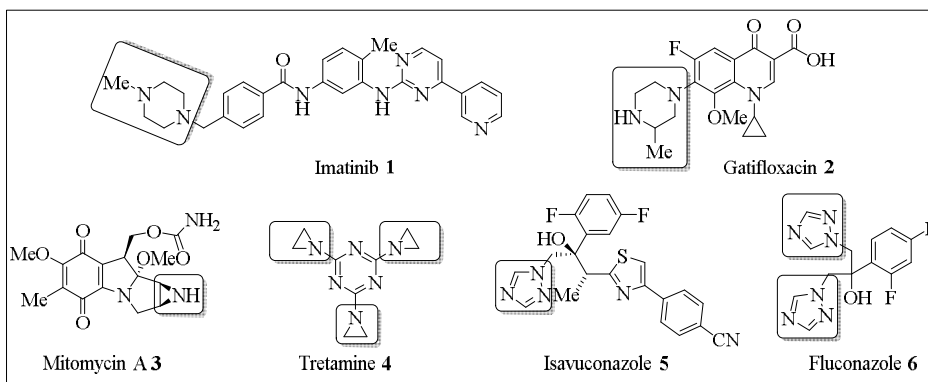


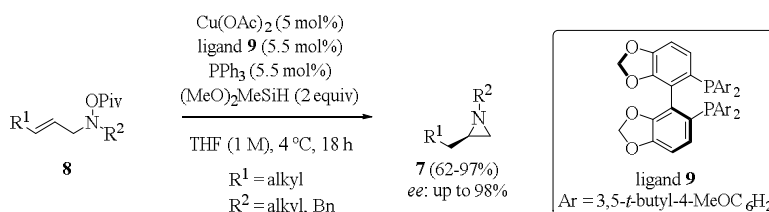
**Figure 1.** Examples of drugs bearing piperazines, aziridines, and triazoles heterocycles.

## 2. Aziridines

Aziridines are highly reactive three-membered saturated nitrogen-containing heterocycles. Due to their ring strain, they can react with different electrophiles and nucleophiles enabling a plethora of chemical transformations that lead to the formation of various chemically and biologically interesting compounds.<sup>22</sup> Although in the past aziridines were considered difficult to synthesize due to their instability, a variety of methodologies have been reported for their preparation such as catalytic, annulation, and cycloaddition reactions, including more sustainable procedures using flow chemistry.<sup>2, 18</sup> Aziridines are useful building blocks for the preparation of more complex heterocycles or amino acids, possessing various biological activities.<sup>23</sup>

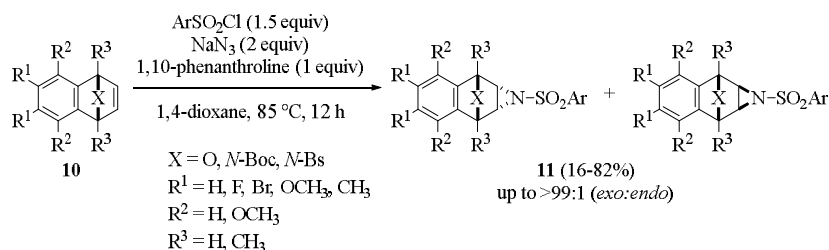
### 2.1. Syntheses of aziridines from alkenes

An innovative methodology for the preparation of alkyl-substituted aziridines **7**, *via* intramolecular hydroamination of allylic hydroxylamine esters **8**, was reported by Buchwald *et al.*<sup>24</sup> The copper catalyst (*S*)-CuCatMix (formed by a combination of copper (II) acetate, ligand **9**, triphenyl phosphine, and dimethoxy(methyl)silane produces *in situ* the copper hydride catalyst fundamental for the reaction, allowing a high degree of enantio- and diastereocontrol (Scheme 1). A wide range of functional groups were tolerated in the scope of the reaction due to the mild reaction conditions.



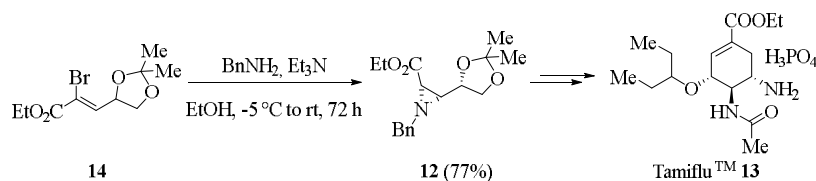
**Scheme 1.** Copper-catalyzed synthesis of aziridine derivatives *via* intramolecular hydroamination of allylic hydroxylamine esters.

Yang and co-workers documented an efficient three-component reaction of oxa(aza)bicyclic alkenes/norbornene **10** in the presence of NaN<sub>3</sub> and arylsulfonyl chlorides, for synthesizing the corresponding aziridines **11** in good yields (up to 82%) with moderate to good *endo/exo* selectivities (up to >99:1 *endo/exo*) (Scheme 2).<sup>25</sup> This protocol requires very simple and mild reaction conditions and is a metal-free catalyzed reaction.



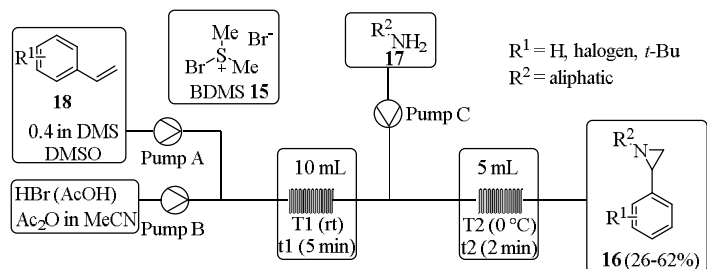
**Scheme 2.** Three-component reaction for preparing aziridines.

Aziridine **12**, reported by Gonnade *et al.*, was used as precursor for the preparation of the well-known Tamiflu<sup>TM</sup> **13**, also called oseltamivir phosphate. In one of the described procedures, *cis*-aziridine **12** was synthesized from vinyl bromide **14** and then used as a chiral synthon (Scheme 3).<sup>26,27</sup>



**Scheme 3.** Synthesis of Tamiflu<sup>TM</sup> **13** via aziridination of vinyl bromide **14**.

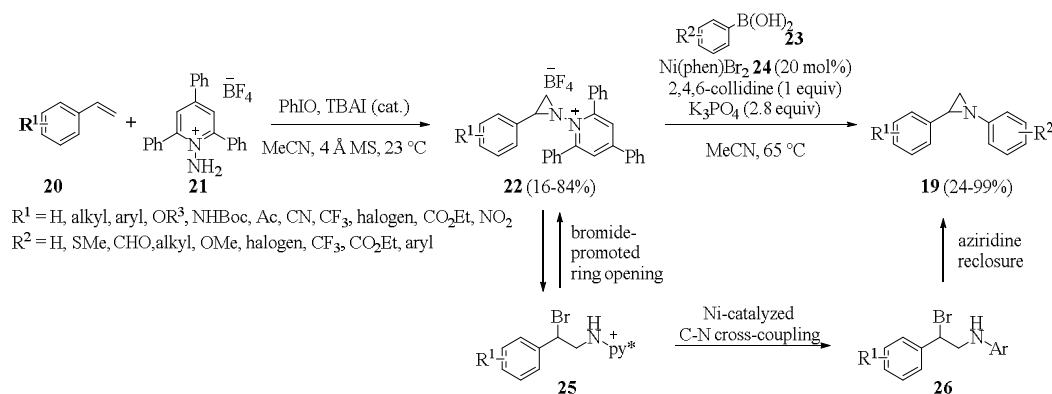
A continuous flow sequence involving bromodimethylsulfonium bromide **15** (BDMS) generation/alkene sulfobromination/aziridination was described by Kappe and co-workers for the preparation of functionalized aziridines **16**.<sup>28</sup> The continuous process allowed the authors to generate BDMS **15** (starting from HBr and DMSO) in a safe manner, which is notable as it is corrosive and sensitive to heat and moisture, releasing molecular bromine (Br<sub>2</sub>) upon contact with water. BDMS **15** was then allowed to react with primary amines **17** and styrene derivative **18** to yield 2-phenyl aziridines **16** (Scheme 4).



**Scheme 4.** Continuous flow bromodimethylsulfonium bromide generation/alkene sulfobromination/aziridination sequence for preparing functionalized aziridines.

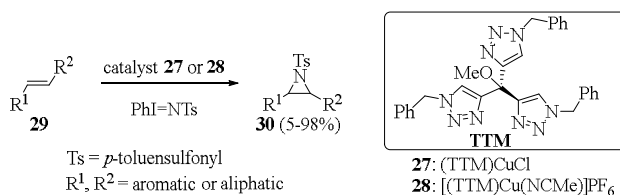
Powers and colleagues reported a two-step procedure for the preparation of *N*-aryl aziridines **19**.<sup>29</sup> In particular, the first step consists of a styrene **20** aziridination with *N*-aminopyridinium reagent **21** to afford *N*-pyridinium aziridines **22** followed by a nickel-catalyzed CN cross-coupling of the *N*-pyridinium aziridines

**22** with aryl boronic acids **23**. The *N*-aminopyridinium reagent **21** acts as a traceless activating group. Mechanistic studies revealed that the aziridine cross-coupling occurs *via* a noncanonical mechanism involving initial aziridine **22** opening by the bromide counterion of the Ni catalyst **24**, which leads to the formation of compounds **25**, followed by CN cross-coupling generating the 2-bromo-2-phenylethyl derivatives **26**, and successive aziridines reclosure (Scheme 5).



**Scheme 5.** Synthesis of *N*-aryl aziridines using *N*-aminopyridinium reagents as traceless activating groups.

A copper-catalyzed aziridination of olefins was documented by Pérez and collaborators, highlighting the important role of the halide characterizing the copper catalyst (Scheme 6).<sup>30</sup> They demonstrated that the employed copper(I) complexes (TTM)CuCl **27** and [(TTM)Cu-(NCMe)]PF<sub>6</sub> **28** (TTM=tris(triazolyl) methane ligand) may play different behaviors, from catalytic and mechanistic points of view, depending on the presence or absence of the chloride ligand bonded to the metal center, fundamental for transforming olefins **29** into aziridines **30**.



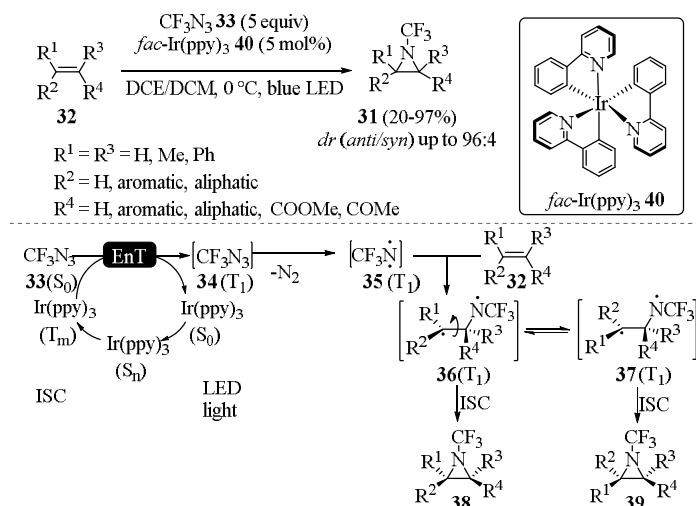
**Scheme 6.** Copper-catalyzed synthesis of aziridine derivatives.

*N*-CF<sub>3</sub>-aziridines **31** were synthesized by Beier *et al.* starting from alkenes **32** *via* iridium-photocatalyzed generation of triplet trifluoromethyl nitrene from trifluoromethyl azide **33**.<sup>31</sup> The authors proposed that in an energy transfer process (EnT), the excited triplet photocatalyst sensitizes CF<sub>3</sub>N<sub>3</sub> **33** into the T<sub>1</sub> state **34** and that a triplet trifluoromethyl nitrene **35** is formed in the photocatalytic process that react with the alkenes **32**. The resulting adduct **36** is in a biradical triplet state with the nitrogen atom connected to one of the carbon atoms of the original double bond. Alkene isomerization, ISC efficiency, or rotation of the CC bond (resulting in conformer **37**) in the newly formed diradical before recombination explain the formation of diastereoisomers **38** and **39** (Scheme 7). In the procedure, *fac*-Ir(ppy)<sub>3</sub> **40** was employed as catalyst.

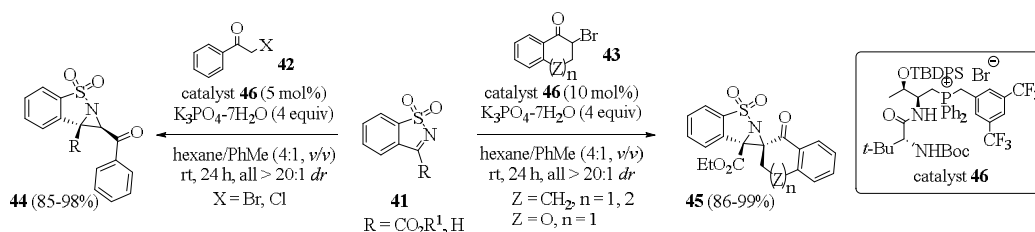
## 2.2. Syntheses of aziridines from imines

Wang and colleagues developed an enantioselective aza-Darzens reaction of cyclic imines **41** with  $\alpha$ -halogenated ketones **42** or **43** for preparing different tri- and tetrasubstituted aziridines, **44** and **45**, respectively, with excellent diastereo- and enantioselectivities (up to >20:1 *dr* and >99.9% *ee*).<sup>32</sup> The reaction proceeds

under mild conditions by using the amino-acid-derived bifunctional phosphonium salt **46** as phase-transfer promoters (Scheme 8).



**Scheme 7.** Iridium-photocatalyzed generation of triplet trifluoromethyl nitrene for the preparation of *N*-CF<sub>3</sub>-aziridines **31**.



**Scheme 8.** Enantioselective aza-Darzens reaction of cyclic imines with  $\alpha$ -halogenated ketones for preparing tri- and tetra-substituted aziridines.

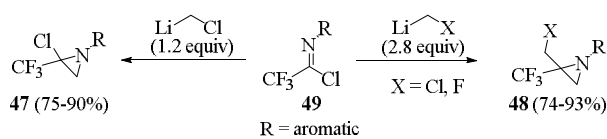
Pace *et al.* documented a telescoped homologation reaction *via* lithium carbenoids (prepared *via* lithium-halogen exchange starting from ICH<sub>2</sub>Cl or ICH<sub>2</sub>F and MeLi-LiBr) for synthesizing mono- **47** and bis-homologated **48** trifluoromethyl-aziridines starting from imines **49**. By adjusting the amount of the carbenoid (either 1.2 or 2.8 equivalents) it was possible to selectively obtain chloro(trifluoromethyl)- **47** or chloromethyl(trifluoromethyl)aziridines **48**, respectively (Scheme 9, path a).<sup>33</sup> Thereafter, the same group, in collaboration with Luisi and collaborators, synthesized a series of rare  $\alpha$ -fluoroaziridines **50** by employing imine derivatives **51** and LiCHFI (prepared from LiN(*i*-Pr)Cy and ICH<sub>2</sub>F) as the homologating agent. The obtained highly functionalized  $\beta$ -fluoroiodoamines **52** were subjected to deprotonation with NaH and after ring closure the desired  $\alpha$ -fluoroaziridines **50** were formed (Scheme 9, path b).<sup>34</sup>

The preparation of spirocyclic aziridines **53** containing a cyclobutane motif was reported by Aggarwal and co-workers in 2023.<sup>35</sup> This two-step one-pot procedure is characterized by the lithiation of a bicyclo[1.1.0]butyl sulfoxide **54** and subsequent addition to a suitable imine **55**. The so-obtained intermediate **56** is cross-coupled with the aryl triflate **57** *via* a C–C  $\sigma$ -bond alkoxy- or aminopalladation, forming the desired aziridines **53** (Scheme 10).

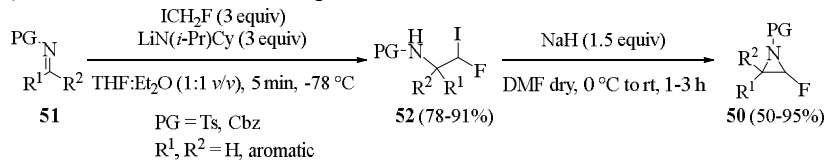
In 2024, Samanta *et al.* described an unprecedented synthesis of sulfamidate-fused aziridines **58**. The products are obtained from the reaction of cyclic *N*-sulfonyl imines **59** with  $\alpha$ -aryl-substituted vinyl azide **60**

upon irradiation of light from blue-LEDs (Scheme 11). The photoactive copper(I)-complex-catalyst was generated *in situ* in presence of ligand **61**.<sup>36</sup>

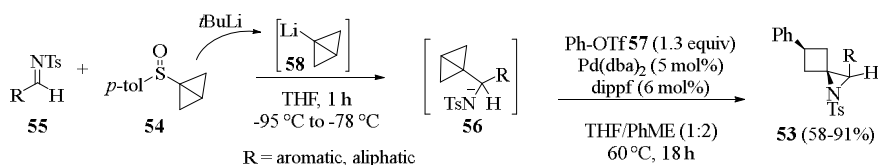
a) Mono- and bishomologated trifluoromethylaziridines



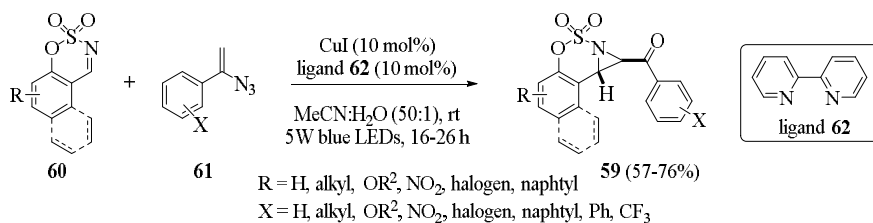
b)  $\alpha$ -Fluoroaziridines: base-mediated ring closure



**Scheme 9.** Lithium carbenoids as homologation agents for preparing of highly functionalized aziridines.



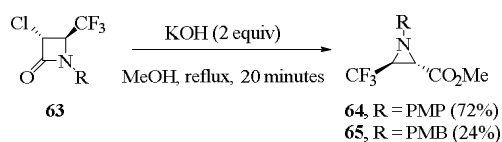
**Scheme 10.** Two-step one pot procedure for the synthesis of spirocyclic aziridines containing a cyclobutane.



**Scheme 11.** Synthesis of sulfamate-fused aziridines starting from cyclic *N*-sulfonyl imines with  $\alpha$ -aryl-substituted vinyl azides.

### 2.3. Miscellaneous

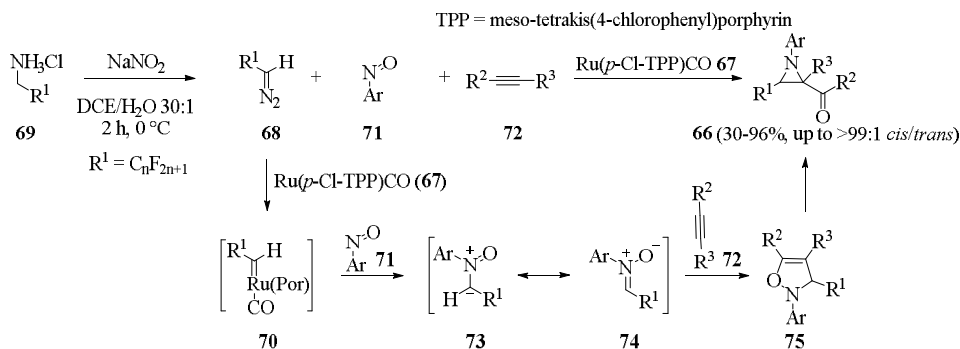
The aziridination of substituted azetidin-2-ones **62** was reported by Dhooghe *et al.* by using KOH in methanol upon ring-rearrangement for the preparation of compounds **63** and **64** (Scheme 12). It is noteworthy, that the starting material **62** can be also transformed into other intriguing heterocycles that are outside of the scope of this chapter.<sup>37</sup>



**Scheme 12.** Synthesis of aziridines *via* ring rearrangement.

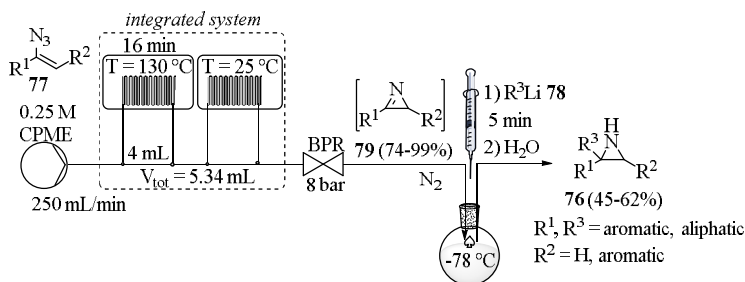
Zhou and collaborators described a multicomponent synthesis for preparing multifunctionalized perfluoroalkyl aziridines **65** in good yields and with moderate to high diastereoselectivity.<sup>38</sup> The reaction

involves coupling between a C–C  $\pi$ -system and numerous nitrogen sources *via* Ru(*p*-Cl-TPP)CO **67** catalysis. The *in situ* generated  $C_nF_{2n+1}CHN_2$  **68** from  $C_nF_{2n+1}CH_2NH_3Cl$  **69** undergoes a sequential nitrene formation/1,3-dipolar-cycloaddition/rearrangement. The ruthenium-perfluoroalkylcarbene intermediate **70** was obtained through the stoichiometric reaction of ruthenium porphyrin **67** and  $C_nF_{2n+1}CHN_2$  **68** (Scheme 13).



**Scheme 13.** Ru-catalyzed synthesis of perfluoroalkyl aziridines.

A sustainable mixed flow-batch methodology was applied by Luisi and co-workers for synthesizing variously functionalized NH-aziridines **76** starting from vinyl azides **77**.<sup>39</sup> The first step of the reaction was carried out under continuous flow, employing the green solvent cyclopentyl methyl ether (CPME), leading to the formation of 2*H*-azirines **79**. The so-obtained 2*H*-azirines **79** solution from the microfluidic system was transferred in a round bottom flask, cooled to  $-78\text{ }^{\circ}\text{C}$  and allowed to react with different lithiated species **78**, in order to obtain the NH-aziridines **76** (Scheme 14).

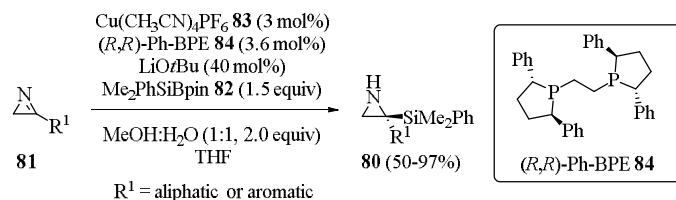


**Scheme 14.** Semicontinuous preparation of NH-aziridines.

Oestreich *et al.* reported in 2023 the preparation of C-silylated unprotected aziridines **80** *via* an enantioselective copper-catalyzed addition of a silicon nucleophile to 3-substituted 2*H*-azirines **81**. A silyl boronic ester **82** was employed as a silicon pronucleophile (Scheme 15) in presence of the copper salt **83** and ligand **84**.<sup>40</sup>

## 2.4 Biological activities of aziridines

Aziridine derivatives display several biological applications.<sup>41</sup> A huge variety of compounds showed activity against different types of oncological diseases.<sup>42</sup> Nevertheless, aziridines possess inhibitory activity towards other biological targets proving to be good cysteine proteases,<sup>43</sup> glucocerebrosidase (GBA),<sup>44</sup> microbial,<sup>44</sup> tuberculosis,<sup>45</sup> and Leishmania inhibitors.<sup>46</sup>



**Scheme 15.** Synthesis of *C*-silylated unprotected aziridines *via* enantioselective copper-catalyzed addition.

#### 2.4.1. Activities of aziridines against oncological targets

The synthesis of *N*-sugar substituted chiral aziridines *via* the Gabriel–Cromwell reaction was described by Bulut and collaborators. The synthesized compounds proved to be promising prodrug candidates for prostate (PC3) and cervical (HeLa) cancers. Among them, derivative **85** showed good activity with an  $IC_{50}$  value of 23.55  $\mu\text{M}$  for PC3 and 25.88  $\mu\text{M}$  for HeLa (Figure 2).<sup>47</sup>

Kalvins and co-workers reported a class of acyl derivatives of aziridine-2-carboxylic acid as weak to moderately active PDIA1 (protein disulfide isomerase) inhibitors. The best activity was observed for compound **86** with an  $IC_{50}$  value of 26.0  $\mu\text{M}$  (Figure 2).<sup>48</sup>

Chloro(trifluoromethyl)aziridine derivatives were documented as selective  $\beta 5$  proteasome inhibitors. The *in vitro* biological activity (enzymatic inhibition and anti-proliferative profile against two leukemia cells lines) was evaluated. The best result was obtained for derivative **87** with an  $IC_{50}$  value of 13.6  $\mu\text{M}$  against the  $\beta 5$  subunit and 25.45  $\mu\text{M}$  against drug-sensitive acute lymphocytic leukemia cells (CCRF-CEM) and 24.08  $\mu\text{M}$  against a multidrug-resistant leukemia sub-cell line (CEM/ ADR5000) (Figure 2).<sup>49</sup> The same group described the inhibitory activity of a class of chloromethyl(trifluoromethyl)aziridines against  $\beta 5$  proteasome subunit. Derivative **88** showed an  $IC_{50}$  value of 9.8  $\mu\text{M}$  (Figure 2).<sup>50</sup>

Cheke *et al.* reported some inhibitors of the stem cell growth factor receptor, known as the c-KIT kinase domain. This is one of the 20 subfamilies of human receptor tyrosine kinases (RTKs) which is one of the main studied targets to fight cancer. The prepared molecules were tested against the NCI-60 human cancer cell lines for a single-dose concentration. The activity of derivative **89**, was evaluated for a five-dose anticancer study showing an  $IC_{50}$  value of 1.47  $\mu\text{M}$  against different breast cancer cell lines (Figure 2).<sup>51</sup>

Calderón-Montañó and collaborators described aziridines  $\beta$ -D-galactopyranoside derivatives as anticancer agents. Compound **90** proved to induce DNA damage showing selective cytotoxicity against different malignant cells in comparison with normal cells. In particular, the highest selectivity was observed for two acute promyelocytic leukemia cell lines, human acute promyelocytic leukemia cells (HL-60) and human acute promyelocytic leukemia cells (NB4) with an  $IC_{50}$  value of 11.1 and 21.4  $\mu\text{M}$ , respectively (Figure 2).<sup>52</sup>

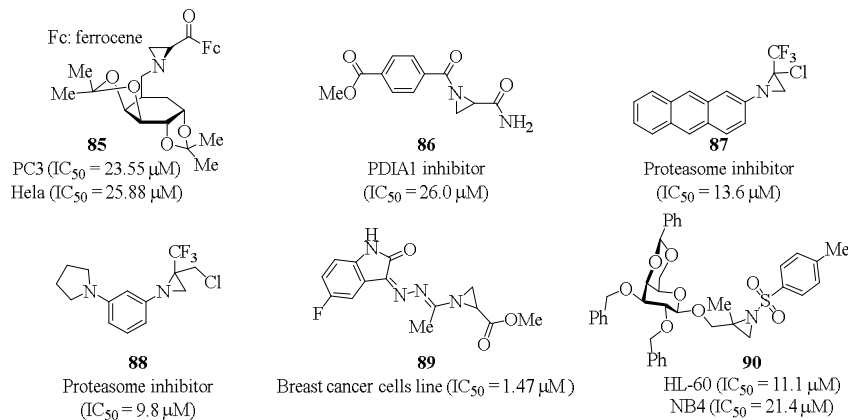


**Figure 2.** Aziridines activities against oncological targets.



### 2.4.2. Different biological targets of aziridines

A series of cyclophellitol aziridine derivatives were reported as promising selective glucocerebrosidase (GBA) inhibitors by Kuo and co-workers. Genetic defects in GBA determine Gaucher disease (GD) and represent a risk factor for developing Parkinson's disease. The best result was shown by compound **91** with an  $IC_{50}$  value of 1.20 nM on human GBA (Figure 3).<sup>44</sup> Schirmeister *et al.* documented a series of aziridine-2,3-dicarboxylate derivatives as potent irreversible inhibitors of cysteine proteases, which are involved in the life cycle of parasites that cause tropical disease such as malaria. Compound **92** proved to be one of the most active with a  $K_i$  value of 4.5  $\mu$ M (Figure 3).<sup>43</sup> The *in vitro* antitubercular activity of aziridines against *Mycobacterium tuberculosis* was evaluated by Gandhimathi and colleagues. Derivative **93** showed a minimum inhibitory concentration (MIC) value of 0.5  $\mu$ g mL<sup>-1</sup> (Figure 3).<sup>45</sup> The antimicrobial activity of functionalized 2-arylaziridines was identified by Luisi *et al.* Selective antibacterial activity against *Enterococcus faecalis* 29212 (MIC=16  $\mu$ g mL<sup>-1</sup>) and an interesting antifungal action against *Candida krusei* 6258 (MIC=16  $\mu$ g mL<sup>-1</sup>) was observed for compound **94** (Figure 3).<sup>53</sup> Sharlow *et al.* described tretazicar (CB1954, 5-(aziridin-1-yl)-2,4-dinitrobenzamide) **95** as a potent inhibitor of the *Leishmania* parasite. *In vivo* studies showed promising activity for curing cutaneous leishmaniasis, which is the most common form affecting humans ( $EC_{50}$ =0.05  $\mu$ M in *L. major* cell-based amastigote) (Figure 3).<sup>54</sup>

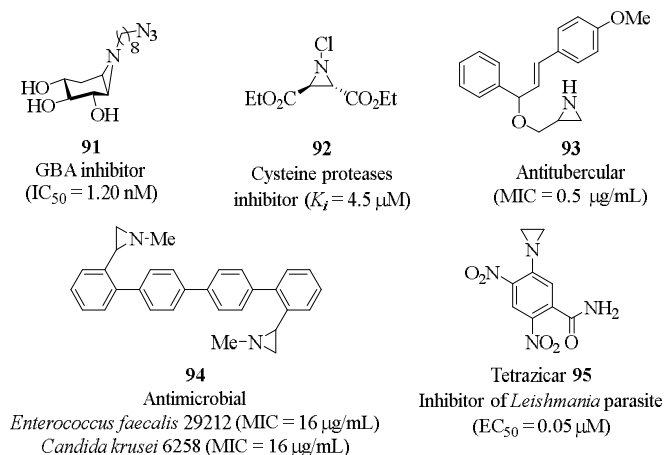
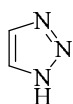


**Figure 3.** Aziridines activities against different biological targets.

### 3. Triazoles

Triazoles are a class of nitrogen-containing heterocycles composed of a five membered ring. They exist in two isomeric forms: 1,2,3-triazoles **96** and 1,2,4-triazoles **97** (Figure 4).<sup>55</sup> Over the years, triazoles have attracted growing interest in the scientific community for their unique features including weak basicity, polarity, metabolic stability, metal binding and hydrogen bonding abilities, which make them a unique scaffold for the design of new therapeutic agents.<sup>56</sup> In addition, the rise of click chemistry have facilitated the access to a variety of substituted 1,2,3-triazoles containing derivatives enabling to use this moiety as a versatile linker between two pharmacophoric units.<sup>57</sup> Due to the exclusive properties of triazoles, several synthetic approaches have been developed exploiting different organic compounds as source of nitrogen.



1,2,3-Triazole **96**



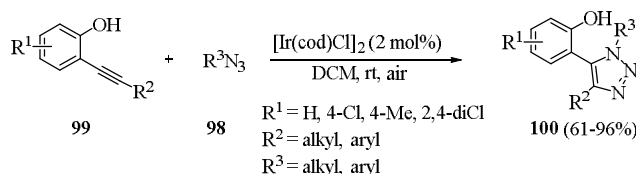
1,2,4-Triazole **97**

**Figure 4.** Structure of 1,2,3- and 1,2,4-triazoles.

### 3.1. Synthesis of 1,2,3-triazoles

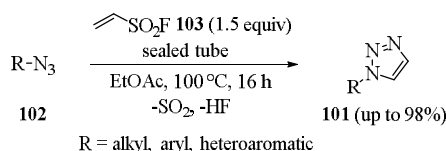
#### 3.1.1. Synthesis of 1,2,3-triazoles from azides

The most used synthetic approach to afford 1,2,3-triazole derivatives is the click chemistry method of Cu-catalyzed azide-alkyne cycloaddition reaction (CuAAC) developed by Sharpless<sup>58</sup> which provides 1,2,3-triazoles in high yields. Over the years, different strategies have been reported to obtain 1,2,3-triazoles from azides. In 2018, Cui and colleagues documented a novel iridium-catalyzed cycloaddition of azides **98** with 2-alkynyl phenols **99** to afford fully substituted triazoles **100** under mild conditions (Scheme 16).<sup>59</sup> The authors assumed that the hydroxyl group of the alkyne acts as directing group allowing the cycloadditions with azides. Concerning the substrate scope, the reaction provides higher yields with aryl-substituted alkynes with respect to alkyl-substituted alkynes.



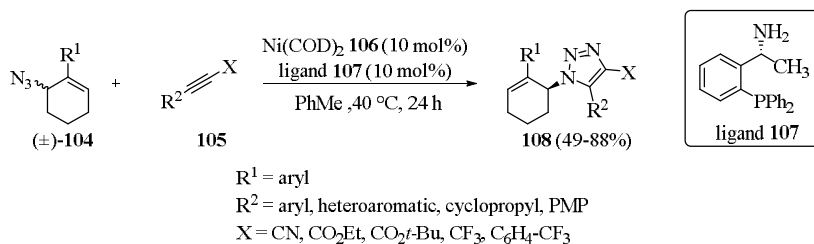
**Scheme 16.** Synthesis of fully substituted 1,2,3-triazole *via* iridium-catalyzed cycloaddition of azides and 2-alkynyl phenols.

A metal-free click protocol to access 1-substituted 1,2,3-triazoles **101** from organic azides **102** and ethenesulfonyl fluoride (ESF) **103** was reported by Moses and co-workers.<sup>60</sup> The reaction consists of a 1,3-dipolar-cycloaddition-elimination between the azides and ESF and occurs in EtOAc under reflux (Scheme 17). These practical metal-free methods displayed broad scope, good functional group tolerability and good to excellent yields.



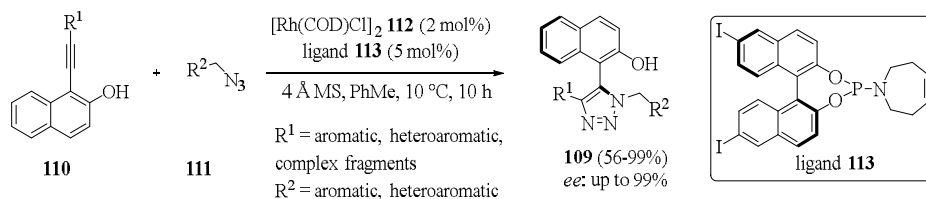
**Scheme 17.** Metal-free click synthesis of 1,2,3-triazoles from organic azides and ESF.

In 2021, Topczewski *et al.* published the first enantioselective triazole synthesis through nickel-catalyzed alkyne-azide cycloaddition (NiAAC) by dynamic kinetic resolution (DKR).<sup>61</sup> The reaction combined allylic azides **104** and EWG-substituted alkynes **105**, which is ideally an alkynonitrile, in presence of  $\text{Ni}(\text{COD})_2$  **106** as catalyst and (*R*)-1-(2-(diphenylphosphanyl)phenyl)ethan-1-amine **107** as ligand (Scheme 18). The DKR is enabled by a spontaneous [3,3]-sigmatropic rearrangement of the allylic azide. Regarding the alkyne scope, arenes with strong EWG reduced regioselectivity. Alkynoates as well as trifluoromethyl alkynes underwent the reaction giving the corresponding products **108**. Exploring the scope of allyl azides revealed that aryl bearing both EWG and EDG are well-tolerated.



**Scheme 18.** Enantioselective synthesis of 1,2,3-triazoles through NiAAC.

Li and co-workers described a challenging atroposelective synthesis of axially chiral 1,4,5-trisubstituted 1,2,3-triazoles **109** *via* the enantioselective Rh-catalysed cycloaddition of internal alkynes **110** and azides **111**.<sup>62</sup> The synthesis occurred in presence of [Rh(COD)Cl]<sub>2</sub> **112** as catalyst, ligand **113** and 4 Å molecular sieves (MS), which increased the enantioselectivity of the reaction (Scheme 19). This method showed high functional group tolerability, moderate to excellent yields, specific regioselectivity and high enantioselectivity.

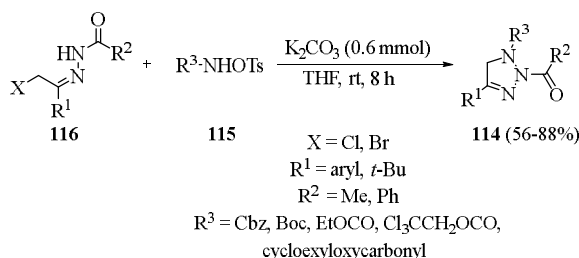


**Scheme 19.** Enantioselective Rh-catalysed cycloaddition of internal alkynes and azides for the synthesis of axially chiral 1,4,5-trisubstituted 1,2,3-triazoles.

### 3.1.2. Synthesis of 1,2,3-triazoles: azide-free approaches

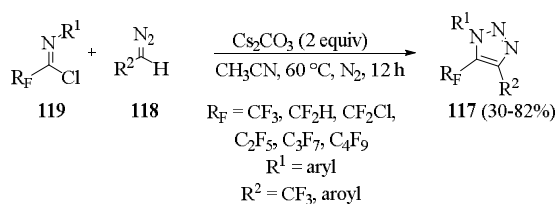
Over the years, 1,2,3-triazoles have been synthesized starting from hydrazones, diazo compounds, and hydrazines as source of nitrogen to avoid the risks associated with the use of high explosive azides.

A green approach to afford 1,2,3-triazoles **114** *via* the K<sub>2</sub>CO<sub>3</sub>-mediated [4+1]-annulation of *N*-acetyl hydrazones **115** with bifunctional amino reagents **116** was developed by Shao and colleagues<sup>63</sup> (Scheme 20). This method provides the desired product from moderate to good yields without the use of azides, metals, organocatalysis or oxidants. Benzyl-*N*-tosyloxycarbamate (CbzNHOTs) was employed as the N1 synthon and the reaction showed good tolerability also with other carbamate derivatives as protecting groups. This strategy proved wide scope allowing different alkyl and aryl substituted 1,2,3-triazole derivatives to be synthesized.



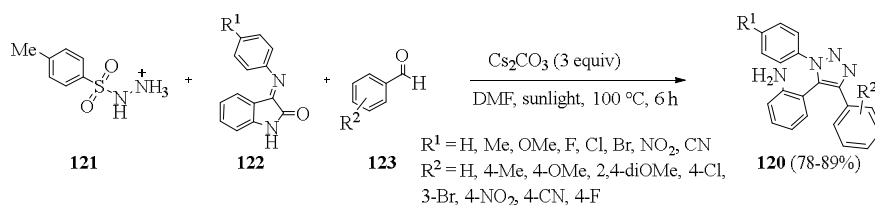
**Scheme 20.** Synthesis of 1,2,3-triazoles *via* the K<sub>2</sub>CO<sub>3</sub>-mediated [4+1] annulation of *N*-acetyl hydrazones.

In 2021, Wu and colleagues documented the synthesis of 5-fluoromethyl-1,2,3-triazoles **117** by base-mediated annulation of diazo compounds **118** with fluorinated imidoyl chlorides **119** (Scheme 21).<sup>64</sup> This metal-, azide-, and CF<sub>3</sub>-free protocol showed broad substrate scope, moderate to good yields under mild conditions and synthetic utility to afford various 5-fluoromethyl-1,2,3-triazole containing derivatives **117**.



**Scheme 21.** Base-mediated annulation of diazo compounds with fluorinated imidoyl chlorides for the synthesis of 5-fluoromethyl-1,2,3-triazoles.

In the same year, Krishna and collaborators documented a photoinduced one-pot three-component synthetic protocol to obtain 1,4,5-trisubstituted-1,2,3-triazoles **120** using tosylhydrazine **121**, isatin Schiff bases **122** and benzaldehydes **123** as starting materials (Scheme 22).<sup>65</sup> The exploration of the substrate scope of isatin Schiff bases and benzaldehydes revealed that both EWG and EDG groups are well tolerated. Under dark conditions, only traces of the product were obtained, demonstrating the key role exerted by the light in promoting the reaction. Overall, this synthetic route allows functionalised regioselective 1,2,3-triazole derivatives to be obtained under mild and simple conditions.

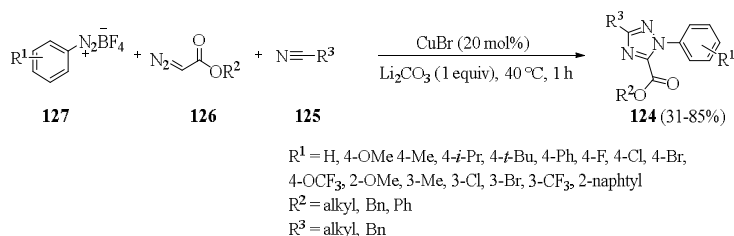


**Scheme 22.** Photo-mediated synthesis of 1,4,5-trisubstituted-1,2,3-triazoles.

### 3.2. Synthesis of 1,2,4-triazoles

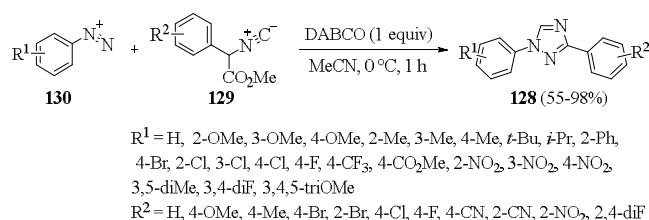
#### 3.2.1. Synthesis of 1,2,4-triazoles from diazonium salts

A common strategy to afford 1,2,4-triazoles consists of the use of diazonium salts and nitriles as starting materials. In this context, Wan et al. reported a novel copper-catalysed three-component reaction to access fully substituted 1,2,4-triazoles **124** via the [3+2]-cycloaddition between nitrile ylides, generated *in situ* from nitriles **125** and diazo compounds **126**, and diazonium salts **127** (Scheme 23).<sup>66</sup> Regarding, the scope with respect to diazo compounds and nitriles, a wide range of functional groups were well tolerated. Instead, concerning the diazonium salts, the efficiency of the reaction decreased with the presence of EWG.



**Scheme 23.** Synthetic route to access fully substituted 1,2,4-triazoles **124** via the [3+2]-cycloaddition of nitrile ylides with diazonium salts.

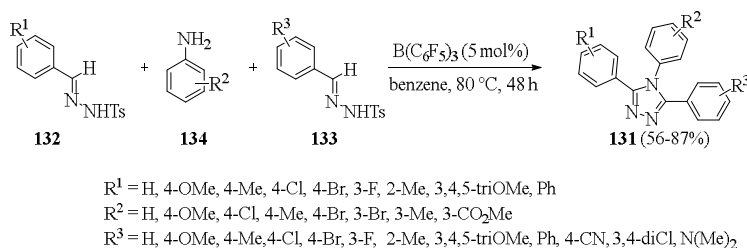
In 2021, Ma and co-workers documented a metal-free approach to obtain 1,3-diaryl-1,2,4-triazoles **128** via decarboxylative annulation of 2-aryl-isocyanoacetates **129** with aryldiazonium salts **130** (Scheme 24).<sup>67</sup> A variety of EWG and EDG on both the aromatic rings of the aryldiazonium salt and the 2-aryl-isocyanoacetates were well tolerated, providing the corresponding products in moderate to good yields.



**Scheme 24.** Metal-free synthesis of 1,3-diaryl-1,2,4-triazoles *via* decarboxylative annulation of 2-aryl-isocyanoacetates with aryldiazonium salts.

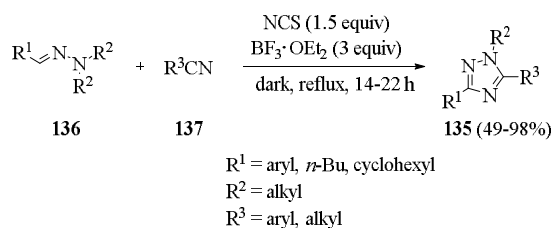
### 3.2.2. Synthesis of 1,2,4-triazoles from hydrazones

A novel procedure for the synthesis of triaryl-1,2,4-triazoles **131** via  $B(C_6F_5)_3$ -catalyzed dehydrogenative cyclization of *N*-tosylhydrazones **132–133** and anilines **134** was reported by Maji *et al.* (Scheme 25).<sup>68</sup> This one-pot metal-free protocol proved to be compatible with a wide array of functional groups allowing the synthesis of both symmetrical and unsymmetrical 3,4,5-triaryl-1,2,4-triazoles **131**.



**Scheme 25.**  $B(C_6F_5)_3$ -Catalyzed dehydrogenative cyclization of *N*-tosylhydrazones and anilines to afford 3,4,5-triaryl-1,2,4-triazoles.

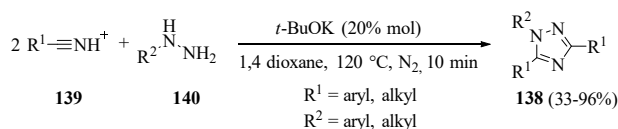
Ueda and colleagues proposed a synthetic method to access multi-substituted 1,2,4-triazoles **135** from *N,N*-dialkylhydrazones **136** and nitriles **137** via formal [3+2]-cycloaddition (Scheme 26).<sup>69</sup> The reaction exploits the ambiphilic reactivity of the iminocarbon of hydrazones, which, under the reaction conditions, generates *in situ* the corresponding hydrazoneyl halide increasing its electrophilicity and thus facilitating the attack of the nitrile nitrogen atom. The reaction displayed wide substrate scope and good functional group tolerability providing a variety of substituted 1,2,4-triazoles from moderate to good yields.



**Scheme 26.** Synthesis of 1,2,4-triazoles via formal [3+2]-cycloaddition of *N,N*-dialkylhydrazones and nitriles.

### 3.2.3. Miscellaneous

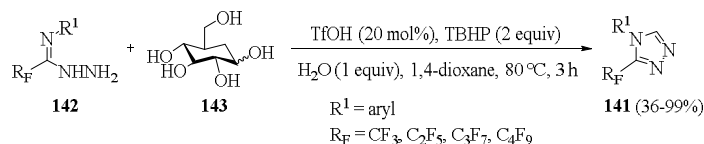
A rapid and efficient protocol to afford 1,3,5-trisubstituted 1,2,4-triazoles **138** through base-mediated annulation of nitriles **139** with hydrazines **140** was developed by Hu and co-workers (Scheme 27).<sup>70</sup> The reaction proceeds via liberation of ammonia gas and allows the introduction of various aromatic and aliphatic groups bearing halo and hetero functional groups, as well as free hydroxyl and amino groups. This strategy requires very simple operating conditions and is a metal-free approach.



**Scheme 27.** Synthesis of 1,3,5-trisubstituted 1,2,4-triazoles via base-mediated annulation of nitriles with hydrazines.

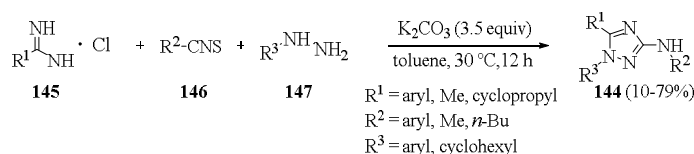
Wu and collaborators proposed a metal-free methodology for the synthesis of 3-trifluoromethyl-1,2,4-triazoles **141** via oxidative cyclization of trifluoroacetimidohydrazides **142** with

D-glucose **143** which is exploited as sustainable C1 synthon to furnish the methine group during the reaction (Scheme 28).<sup>71</sup> This synthetic procedure offers several advantages such as mild conditions, glucose as C1 synthon which provides a readily available reagent from biomass, scalability and wide substrate scope.



**Scheme 28.** Synthesis of 3-trifluoromethyl-1,2,4-triazoles *via* oxidative cyclization of fluorinated acetimidohydrazides with D-glucose.

A green three-component protocol to access fully substituted 1*H*-1,2,4-triazol-3-amines **144** was described by Zheng and colleagues.<sup>72</sup> The reaction is a [2+1+2]-addition occurring *via* the desulfurization and deamination condensation of amidines **145**, isothiocyanates **146**, and hydrazines **147** (Scheme 29). The reaction showed high functional group tolerability, requires only mild conditions and is environmentally friendly.



**Scheme 29.** Green three-component protocol for the synthesis of 1*H*-1,2,4-triazol-3-amines from amidines, isothiocyanates, and hydrazines.

### 3.3. Biological applications of triazoles

Triazoles are versatile scaffolds in medicinal chemistry as the presence of three nitrogen atoms allows a wide range of structural modifications resulting in the obtainment of compounds endowed with several therapeutic effects.<sup>55</sup> Triazoles are well known for their antifungal properties; currently, the most used antifungals agents (such as itraconazole **148**, fluconazole **6**, voriconazole **149**, and posaconazole **150**, Figure 5) bear the 1,2,4-triazole moiety. They act by inhibiting the P450 sterol 14 $\alpha$ -demethylase enzyme (CYP51) through coordination of the heme iron by the free nitrogen of the triazole ring.<sup>73</sup> The impairment of CYP51 activity prevents the conversion of lanosterol into ergosterol, which constitutes the main component of the fungal cell membrane.<sup>74</sup>

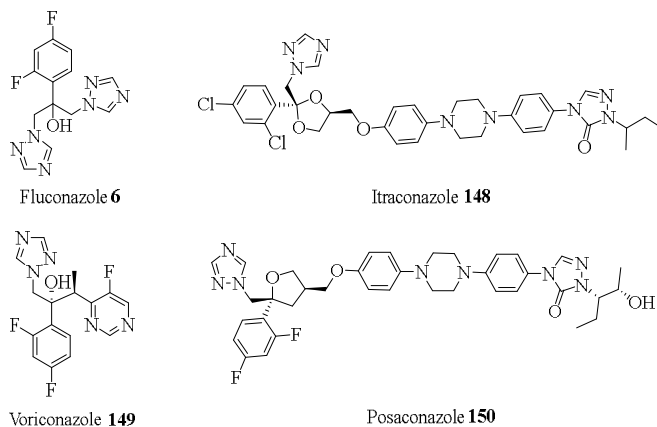


**Figure 5.** Triazole-containing antifungal compounds currently used in therapy.

Despite the high therapeutic index of triazoles, their use is often limited by antifungal drug resistance, which is becoming a worldwide emergency.<sup>75</sup> This has prompted researchers to find new therapeutic solutions. In this scenario, Yan and colleagues described the antifungal properties of a new series of triazole-containing derivatives,<sup>76</sup> which were screened against seven common pathogenic fungi. Compound **151** (Figure 6) revealed to be one of the most promising derivatives showing good inhibitory activity values on some of the tested fungi. In addition, derivative **151** proved to be active against some fluconazole-resistant strains and inhibited the growth of *C. albicans* SC5314 by affecting biofilm formation. GC-MS analysis revealed the involvement of Cyp51 by derivative **151** which also displayed low cytotoxicity, low hemolytic activity, and good pharmacokinetic properties. *In vivo* studies performed on a *G. mellonella* infection model confirmed the antifungal properties of compound **151**.

In 2018, Xu and colleagues adopted a hybridization strategy to develop new antitubercular agents by synthesizing a new class of isatin-propylene-1*H*-1,2,3-triazole-4-methylene-moxifloxacin derivatives that were tested against MTB H<sub>37</sub>Rv and MDR-TB which is resistant to the commonly used drugs moxifloxacin (MXF), rifampicin (RIF) and isoniazid (INH).<sup>77</sup> The most potent compound **152** (Figure 6) showed excellent antitubercular activity on both strains with MIC values of 0.05 µg/mol and 0.06 µg/mol on MTB H<sub>37</sub>Rv and MDR-TB respectively, exhibiting a better or comparable activity with respect to the reference drugs MXF, RIF and INH (MIC=0.10 µg/mol, 0.39 µg/mol and 0.05 µg/mol, respectively on MTB H<sub>37</sub>Rv).

Triazole has been widely exploited to design α-glucosidase inhibitors as new antidiabetic agents. α-Glucosidase is an enzyme implicated in the digestion of carbohydrates as it converts unabsorbed oligosaccharides and disaccharides in absorbable monosaccharides leading to postprandial hyperglycaemia in type II diabetes mellitus (T2DM) patients. Basing on this, inhibiting α-glucosidase activity provides an effective strategy for the management of postprandial hyperglycaemia in T2DM.<sup>78</sup> In this context, Wang and colleagues designed a novel class of xanthone-triazole derivatives as α-glucosidase inhibitors.<sup>79</sup> The most potent compound **153** (Figure 6) showed an IC<sub>50</sub> value of 2.06 µM resulting to be more potent than 1-deoxynojirimycin (IC<sub>50</sub>=59.50 µM) employed as positive control. Kinetic studies revealed that derivative **153** acts as non-competitive inhibitor of α-glucosidase. In addition, compound **153** displayed low cytotoxicity in LO2 cells and the ability to promote glucose uptake in HepG2 cell line, thus exerting an additional mechanism to regulate blood glucose level in T2DM.

Triazole-containing compounds proved to be effective on neurodegenerative disorders. In 2020, De Luca and co-workers reported the *in silico* driven discovery of compound **154** (Figure 6) which displayed the ability to reduce α-synuclein (α-syn) aggregation *in vitro*.<sup>80</sup> The aggregation of α-syn in toxic oligomers and fibrils is a mechanism involved in the neurodegeneration associated with Parkinson's disease (PD) and its inhibition by small molecules represents a promising disease-modifying strategy for reducing or blocking the neurodegenerative process.<sup>81</sup> Structural modifications of derivative **154**, consisting of the replacement of the cinnamic moiety with an ester group, led to the obtainment of compound **155** (Figure 6) which showed neuroprotective effects on a mouse model of PD ameliorating the typical motor symptoms associated to this pathology.<sup>82</sup>

Triazoles often occur in antibacterial and antiviral agents. In 2023, Kumari *et al.* reported the design of novel isatin-semicarbazone tethered 1,2,3-triazole hybrids that were screened against different bacterial strains.<sup>83</sup> Among the synthesized compounds, derivative **156** showed an interesting antibacterial profile (Figure 6) displaying the ability to inhibit *E. coli* (MIC=0.0069 µM) and *P. aeruginosa* (MIC=0.0069 µM) growth with better potencies if compared to the standard ciprofloxacin (MIC of 0.0094 µM on both *E. coli* and *P. aeruginosa*). Furthermore, compound **156** showed also antifungal properties against *C. albicans* (MIC=0.0138 µM) and *R. oryzae* (MIC=0.0138 µM) proving to be more effective than fluconazole used as standard (MIC values of 0.0408 µM on both *C. albicans* and *R. oryzae*). Derivative **156** was also able to inhibit biofilm formation in *P. aeruginosa*.

In the same year, Ekins and colleagues described the anti-HIV activity of a new class of *N*-phenyl-1-(phenylsulfonyl)-1*H*-1,2,4-triazol-3-amine acting as non-nucleoside transcriptase inhibitors (NNRTI).<sup>84</sup> The most promising compound 12126065 **157** (Figure 6) showed good antiviral properties in TZM cells against both wild-type HIV (IIIB) (IC<sub>50</sub>=0.24 nM) and A17 mutant (EC<sub>50</sub>=1.30 nM). In addition, derivative **157** proved to be effective also on other clinically relevant HIV mutants including Y181C (IC<sub>50</sub>=3.7 nM), L100I (IC<sub>50</sub>=18 nM), and K103N (IC<sub>50</sub>=2.1 nM). *In vitro* assays confirmed the ability of compound **157**

to target HIV reverse transcriptase by inhibiting its activity with an  $EC_{50}$  value of  $0.23\ \mu\text{M}$ . Differently from other NNRTIs currently used in therapy, **157** did not exhibit significant neurotoxicity *in vivo* up to  $10\ \mu\text{M}$  with a  $TC_{50}$  value higher than  $100\ \mu\text{M}$ .

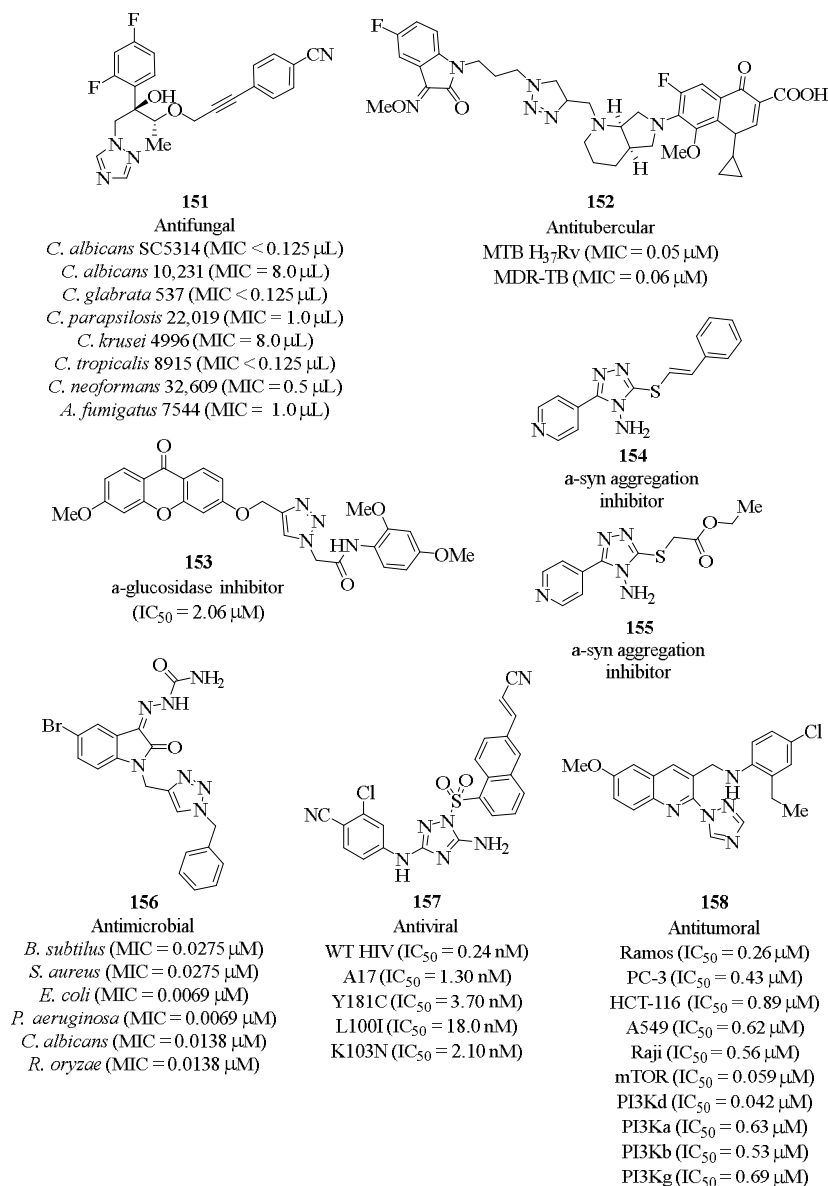


**Figure 6.** Triazoles derivatives endowed with pharmacological activity against multiple targets.

Triazole derivatives have also been used to develop novel anticancer agents. In this context, Duan *et al.* designed a new series of 6-methoxy-2-(1*H*-1,2,4-triazol-1-yl)-quinolin-3-methylene analogues as dual mTOR/PI3K $\delta$  inhibitors.<sup>85</sup> Both proteins are kinases involved in cellular pathways regulating cell growth and survival thus playing crucial roles in cancer.<sup>86</sup> The simultaneous inhibition of mTOR and PI3K $\delta$  is important



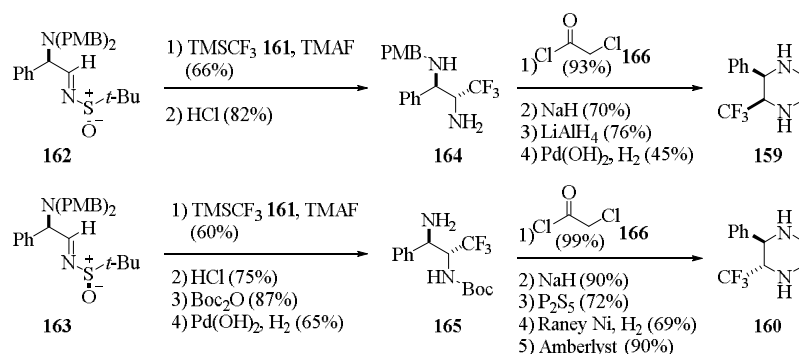
to avoid resistance caused by the reactivation of PI3K by the negative feedback loop of mTOR. Among the synthesized derivatives, compound **158** (Figure 6) exhibited the highest antitumoral activity on Ramos cells with an  $IC_{50}$  value of 0.26  $\mu$ M proving to be more potent than dactolisib ( $IC_{50}$ =0.76  $\mu$ M) used as reference. Furthermore, **158** retained its cytotoxic effect on other cancer cell lines including PC-3 ( $IC_{50}$ =0.43  $\mu$ M), HCT-116 ( $IC_{50}$ =0.89  $\mu$ M), A549 ( $IC_{50}$ =0.62  $\mu$ M), and Raji ( $IC_{50}$ =0.56  $\mu$ M), while being inactive on non-cancerous Vero cells ( $IC_{50}$ >100  $\mu$ M). Enzymatic tests revealed that the cytotoxic effect was related to the dual inhibition of mTOR ( $IC_{50}$ =0.059  $\mu$ M) and PI3K $\delta$  ( $IC_{50}$ =0.042  $\mu$ M) activities. Interestingly, this compound resulted to be selective towards PI3K $\delta$  over the other PI3K isoforms namely PI3K $\alpha$  ( $IC_{50}$ =0.63  $\mu$ M), PI3K $\beta$  ( $IC_{50}$ =0.53  $\mu$ M) and PI3K $\gamma$  ( $IC_{50}$ =0.69  $\mu$ M). Western blot analysis revealed that **158** blocks the PAM cascade while the Annexin-V assay highlighted its capability to promote apoptosis leading to cell death.<sup>85</sup>

#### 4. Piperazines

Piperazine is a six-membered heterocycle bearing two nitrogen atoms in the 1- and 4-position, largely diffused in chemistry. It is the third most commonly used *N*-heterocycle (ranked right behind piperidine and pyridine) in small-molecule pharmaceuticals.<sup>87</sup> The presence of the two nitrogen atoms, at positions 1 and 4 of the ring, allows a huge variety of substitutions for the synthesis of pharmaceutical ingredients, most of them possessing substitutions on either both nitrogen atoms or on a single nitrogen atom. Piperazine is mainly used as a linker to connect two portions of a drug or as an accessory to modulate the drug's physicochemical properties. Indeed, it provides a large polar surface area, relative structural rigidity, and additional hydrogen-bond acceptors and donors, which often lead to enhanced target affinity and specificity and improved water solubility, oral bioavailability, and ADME (absorption, distribution, metabolism, and excretion) properties.<sup>88</sup> Due to the importance of such heterocycle, several synthetic methodologies have been developed for its preparation.<sup>20</sup>

##### 4.1. Syntheses of piperazines *via* ketopiperazine reduction and *N*-alkylation

Fustero *et al.* reported a multistep procedure for the synthesis of enantiomerically pure *cis*- and *trans*-2-phenyl-3-(trifluoromethyl)piperazines **159**-**160**.<sup>89</sup> The key step of this synthetic protocol is the stereoselective nucleophilic addition of the Ruppert-Prakash reagent (TMSCF<sub>3</sub>) **161**<sup>90,91</sup> to the  $\alpha$ -amino *tert*-butylsulfinimines **162**-**163**, leading to the formation of **164** and **165**, harnessing the stereoselective addition to Ellman's<sup>92</sup> auxiliary (Scheme 30).

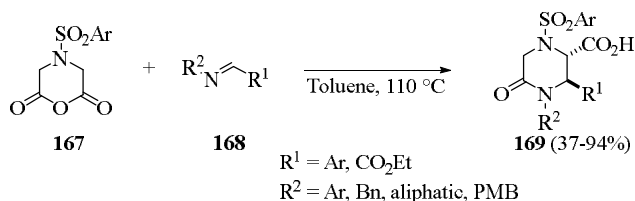


**Scheme 30.** Synthesis of enantiomerically pure *cis*- and *trans*-2-phenyl-3-(trifluoromethyl)piperazine.

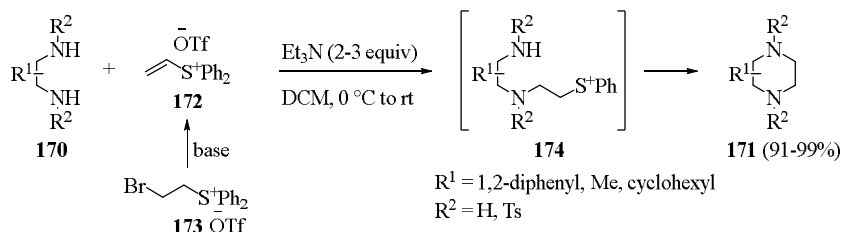
The Castagnoli-Cushman reaction,<sup>93</sup> starting from nitrogen-bearing glutaric anhydride analogues **167** and imines **168** as coupling partners, was reported by Krasavin and co-workers for the preparation of various ketopiperazines **169**. Substituents were reported to be arranged in a *trans*-manner because of stereoselectivity (Scheme 31).<sup>94</sup>

Aggarwal and collaborators described the alkylation of 1,2-diamine derivatives **170** for the synthesis of piperazines **171** *via* a sequence of conjugate addition to vinyl sulfonium salts **172** followed by an intramolecular ring closure.<sup>95</sup> The diphenyl vinyl sulfonium salt **172** can be synthesized *via* a base-promoted

elimination of the corresponding bromoethylsulfonium salt **173**. It reacts with both free and tosyl-protected 1,2-diamines **170** under very mild reaction conditions with triethylamine as base and at 0 °C to room temperature generating intermediates **174** which are then transformed into derivatives **171** (Scheme 32).

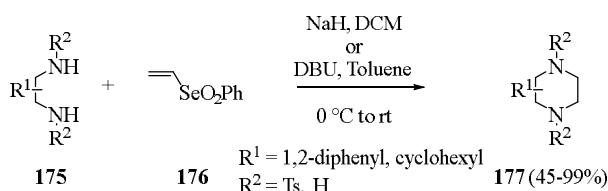


**Scheme 31.** Synthesis of ketopiperazine *via* Castagnoli-Cushman reaction.



**Scheme 32.** Alkylation of 1,2-diamine for the synthesis of piperazines.

*N*-Protected-1,2-diamines **175** were allowed to react in the presence of vinyl selenone **176** by Tiecco and co-workers for the preparation of piperazine derivatives **177** (Scheme 33).<sup>96</sup> The reaction is a one-pot procedure occurring in the presence of a base, *via* a simple and novel application of the Michael-initiated, ring-closure (MIRC) reactions.



**Scheme 33.** Synthesis of piperazines from diamines and vinyl selenone.

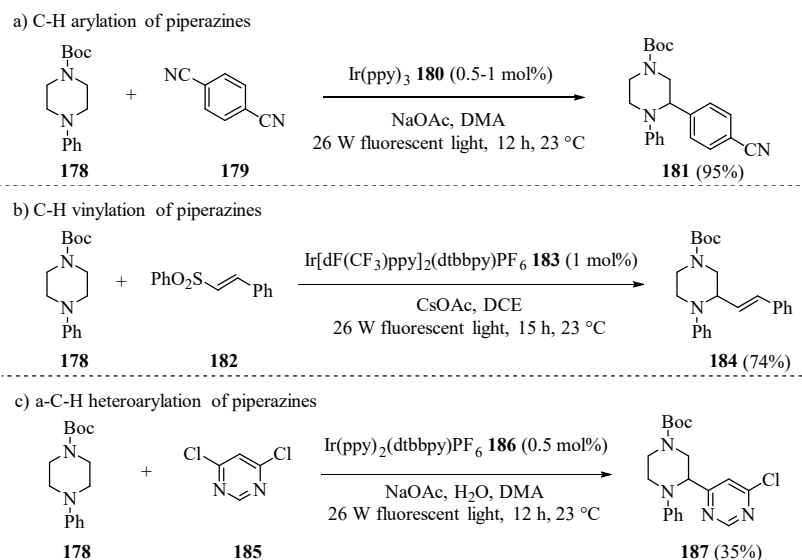
#### 4.2. Syntheses of piperazines *via* catalysis

A photoredox catalysis approach was employed by MacMillan and colleagues for preparing CH functionalized piperazines. *N,N*-disubstituted piperazine **178** was reacted with 1,4-dicyanobenzene **179** in presence of Ir(ppy)<sub>3</sub> **180** as photocatalyst forming piperazine **181** (Scheme 34, path a).<sup>97</sup> This protocol was further extended to CH vinylation of piperazine **178** by using vinyl sulfones **182**; the catalyst system was changed to Ir<sup>III</sup>[dF(CF<sub>3</sub>)ppy]<sub>2</sub>(dtbbpy)PF<sub>6</sub> **183**/CsOAc/DCE to provide the product **184** with high *E*-selectivity (Scheme 34, path b).<sup>98</sup> Finally, MacMillan and co-workers proposed the  $\alpha$ -CH heteroarylation of piperazine **178** in presence of 4,6-dichloropyrimidine **185** by using Ir<sup>III</sup>(ppy)<sub>2</sub>(dtbbpy)PF<sub>6</sub> **186** as catalyst for the preparation of compound **187** (Scheme 34, path c).<sup>99</sup>

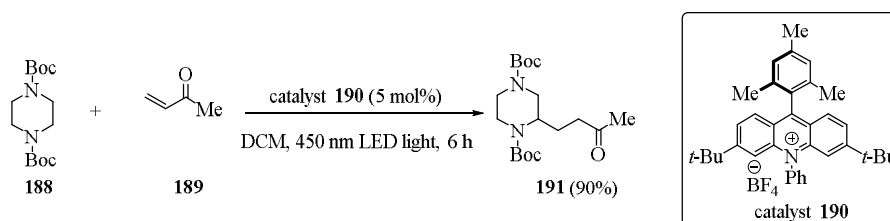
Nicewicz *et al.* reported the CH alkylation of carbamate-protected piperazine **188** in presence of  $\alpha,\beta$ -unsaturated carbonyl derivative **189** using the substituted acridinium salt **190** as organic photocatalysts for generating piperazine **191** (Scheme 35).<sup>100</sup> This methodology was then further improved and extended to different substituted piperazines in presence of several carbonyl compounds.<sup>101</sup>

SnAP (stannyl amine protocol) chemistry was developed by Bode and co-workers as a convergent method for the synthesis of piperazines **192** from aldehydes **193**. The tin-substituted starting materials **194**,

readily synthesized from the corresponding diamines and tributyl(iodomethyl)stannane, allow a combined cyclization/CC bond addition to imines in order to form the desired piperazine derivatives **192**. In this methodology, copper is employed, which oxidizes the CSn bond to form a heteroatom-stabilized  $\alpha$ -aminyl radical, which then undergoes cyclization with the intermediate imine **195** (Scheme 36, path a).<sup>102-104</sup> Due to the large amount of copper employed and the subsequent problem of using the methodology at industrial level, Bode *et al.* improved the procedure by using 4:1 HFIP/CH<sub>3</sub>CN instead of 4:1 DCM/HFIP and catalytic amount of copper. The improvement of this pathway allowed the scope of the reaction to be extended.<sup>105</sup> Later on, ketones were employed in order to synthesize poly-carbon-substituted and spirocyclic piperazines.<sup>106</sup> The methodology was then further ameliorated by exchanging tin (due to its toxicity) with silicon (silicon amine protocol - SLAP) and copper with Ir<sup>III</sup>(ppy)<sub>2</sub>(dtbbpy)PF<sub>6</sub> **186** as a promoter of the reaction under blue light irradiation (Scheme 36, path b).<sup>107</sup> Compounds **196** were used as starting materials leading to the formation of intermediates **197** and final cyclization to obtain the desired products **198**.



**Scheme 34.** CH Functionalization of piperazines.

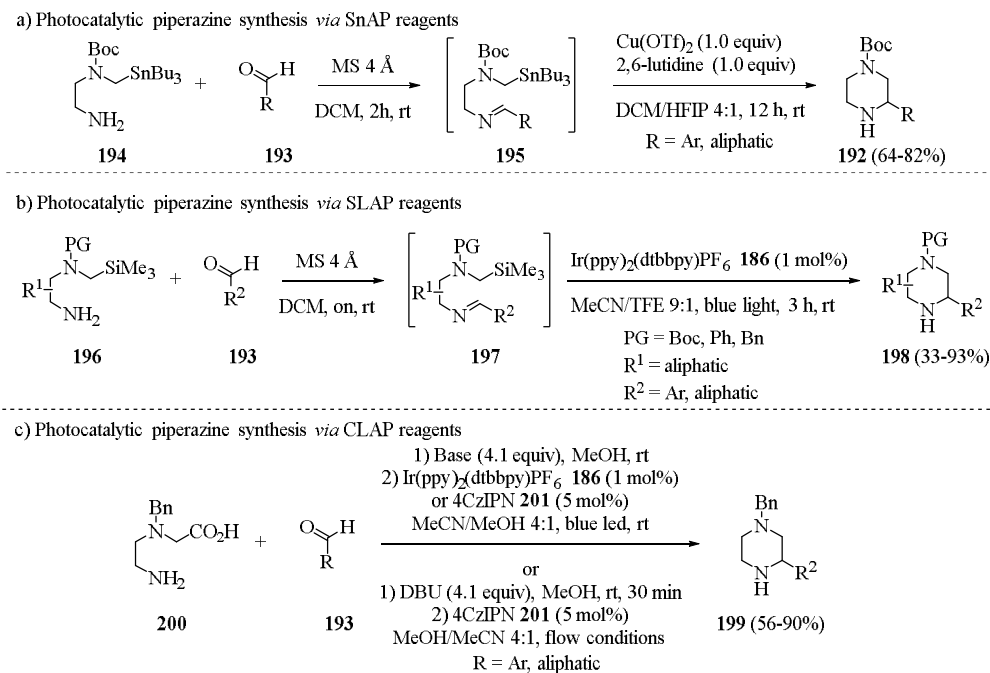


**Scheme 35.** CH Alkylation of carbamate-protected piperazines.

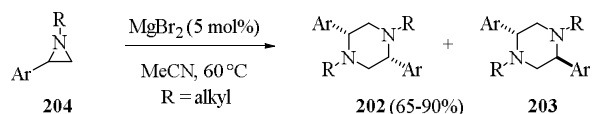
Furthermore, Bigot and collaborators proposed a photoredox CLAP protocol (CarboxyLic Amine Protocol) for the synthesis of C2-functionalized piperazines **199** by using a variety of aldehydes **193** and amino-acid-derived diamines **200**. Ir<sup>III</sup>(ppy)<sub>2</sub>(dtbbpy)PF<sub>6</sub> **186** was employed as photoredox catalyst or in alternative, the organic photocatalyst, carbazolyl dicyanobenzene **201** (4CzIPN) in presence of a base. The substitution of KOH with DBU allowed to perform the reaction in continuous flow, due to the formation of a precipitate when KOH was employed (Scheme 36, path c).<sup>108</sup>

### 4.3. Miscellaneous

Luisi and co-workers documented in 2012 the preparation of 2,5-disubstituted piperazines **202-203** via Lewis acid-catalyzed dimerization of aziridines **204**. By using 5 mol% of magnesium bromide, non-activated *N*-alkyl arylaziridines **204** underwent ring opening with another aziridine followed by ring-closure to afford the desired compounds **202-203**. The so-obtained 2,5-disubstituted piperazines resulted in a mixture of stereoisomers due to the lack of stereochemical control of the process (Scheme 37).<sup>109</sup>

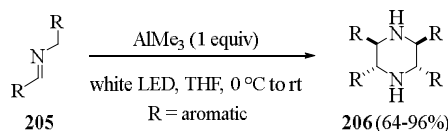


**Scheme 36.** SnAP, SLAP, and CLAP chemistry for the synthesis of CH functionalized piperazines.



**Scheme 37.** Synthesis of 2,5-disubstituted piperazines via aziridine ring opening.

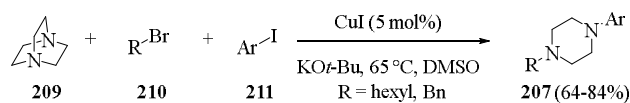
Azomethine ylides **205** possessing aromatic substituents were converted by Mendoza *et al.* into piperazine derivatives **206** in presence of trimethylaluminum under white LED lamps.<sup>110</sup> This is another example of dimerization for synthesizing piperazines. Not only symmetrical compounds but also unsymmetrical ones, bearing imidazole and pyridine or pyrazine groups, were produced and obtained as single regioisomers (Scheme 38).



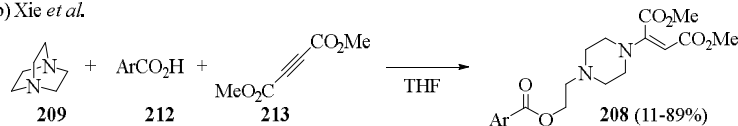
**Scheme 38.** Dimerization of azomethine ylides for preparing piperazines.

Yavari *et al.*<sup>111</sup> (Scheme 39, path a) and Xie and co-workers<sup>112</sup> (Scheme 39, path b) were able to prepare unsymmetrical *N*-substituted piperazines **207-208** by using 1,4-diazabicyclo[2.2.2]octane **209** (DABCO). In the first case alkyl bromides **210** and aryl iodides **211** were employed, whereas Xie and collaborators used carboxylic acid derivatives **212** and dimethyl but-2-ynedioate **213**. Both these methodologies are limited to the synthesis of *N*-substituted piperazines due to the use of DABCO **209** as starting material.

a) Yavari *et al.*

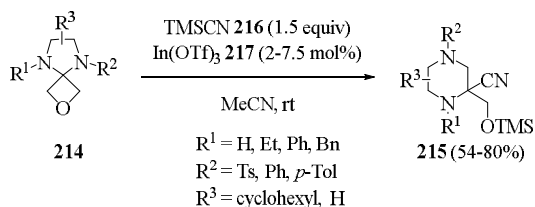


b) Xie *et al.*



**Scheme 39.** 1,4-Diazabicyclo[2.2.2]octane for preparing different substituted piperazines.

3-Oxetanone-derived spirocycles **214**, prepared from the suitable 1,2-diamine derivatives and 3-oxetanone, were employed by Carreira and co-workers for the synthesis of piperazines **215**.<sup>113</sup> This is a ring expansion methodology which proceeds under Strecker reaction<sup>114</sup> conditions in presence of trimethylsilyl cyanide **216** and indium(III) triflate **217** (Scheme 40).



**Scheme 40.** Ring expansion of 3-oxetanone-derived spirocycles for preparing piperazines.

#### 4.4. Biological activities of piperazine derivatives

The piperazine ring has been largely exploited for the design of compounds endowed with multiple therapeutic effects.

In 2018, Li and colleagues reported the antidepressant-like activity of a new series of aralkyl piperazine derivatives targeting the serotonin receptors 5-HT<sub>1A</sub>/5-HT<sub>7</sub> and the serotonin transporter SERT.<sup>115</sup> The simultaneous inhibition of various 5-HT receptors subtypes and serotonin reuptake represents a valuable strategy for the treatment of depression.<sup>116</sup> Among the synthesized derivatives, compound **218** (Figure 7) proved to be the most potent displaying  $K_i$  values of 28 nM and 3.3 nM on 5-HT<sub>1A</sub> and 5-HT<sub>7</sub>, respectively and inhibiting the reuptake (RUI) with an  $\text{IC}_{50}$  value of 25 nM. The antidepressant activity of **218** was also evaluated *in vivo* through two animal behavioural tests, FST and TST models. In both tests, this derivative showed a dose-dependent reduction of the immobility time thus confirming its efficacy *in vivo*. In addition, compound **218** displayed good pharmacokinetics properties and an acceptable hERG profile.<sup>115</sup>

In the same year, Popik *et al.* documented the antipsychotic effects of a novel set of multitarget azinesulfonamides of cyclic amine derivatives bearing the aryl-piperazine pharmacophore.<sup>117</sup> Derivative **219** (Figure 7) showed an interesting polypharmacological profile acting as partial agonist on 5-HT<sub>1A</sub> ( $\text{EC}_{50}$ =28.3 nM), antagonist on 5-HT<sub>2A</sub> ( $K_b$ =2.3 nM), 5-HT<sub>7</sub> ( $K_b$ =3.4 nM), D<sub>2</sub> ( $K_b$ =3 nM), and D<sub>3</sub> ( $K_b$ =92 nM) receptors, as well as SERT binding inhibitor ( $K_i$ =76 nM). *In vivo* studies assessed the ability of compound **219** to alleviate both the positive and the negative symptoms associated with psychosis. In particular, this multitarget ligand was able to reverse the PCP-induced hyperactivity and avoidance behaviour in the CAR test and the social

interaction deficit in a ketamine model. Moreover, compound **219** exhibited pro-cognitive effects, no tendency to induce catalepsy, no cardiotoxic effects and low hyperprolactinemia liability.

Kiec-Kononowicz and collaborators designed a new series of *tert*-pentylphenoxyalkylpiperazines targeting histamine H<sub>3</sub> receptors (hH<sub>3</sub>R) as anticonvulsant agents.<sup>118</sup> The most promising derivative, compound **220** (Figure 7), showed high affinity towards hH<sub>3</sub>R with a *K<sub>i</sub>* value of 37.8 nM acting as antagonist in the functional bioassay. *In vivo* studies performed on the maximal electroshock-induced seizure model demonstrated that **220** was able to induce anticonvulsant effects in mice. In addition, compound **220** was able to penetrate into CNS and exhibited pro-cognitive properties in the passive avoidance test.

In 2021, Almansa and collaborators developed a new series of piperazine-containing derivatives endowed with analgesic effects by acting as dual ligands against the  $\mu$ -opioid (MOR) and  $\sigma_1$  ( $\sigma_1$ R) receptors.<sup>119</sup> This multimodal strategy allows the potentiation of the opioid analgesia with the inhibition of  $\sigma_1$ R which proved to be effective on neuropathic pains where opioids are less efficacious. Derivative **221** (Figure 7) was identified as promising lead compound exhibiting partial agonistic activity on MOR receptor (*E<sub>max</sub>* 74%) and the ability to inhibit  $\sigma_1$ R with a *K<sub>i</sub>* value of 108 nM. Compound **221** showed an adequate pharmacokinetic profile and low hERG inhibition. The analgesic effect of **221** was confirmed *in vivo* in acute and chronic pain mice models. Interestingly, compound **221** exerted less opioid-typical side effects including tolerance and constipation with respect to oxycodone.

Lu *et al.* reported the discovery of piperazine containing compounds effective against *Mycobacterium tuberculosis* (MTB).<sup>120</sup> Compound **222** (Figure 7) showed an excellent inhibitory profile *in vitro* against both the drug-sensitive MTB strain H37Rv (MIC<0.016  $\mu$ g/mL) and multidrug-resistant clinical strains, MDR-MTB 16995 (MIC<0.016  $\mu$ g/mL) and MDR-MTB 16833 (MIC<0.016  $\mu$ g/mL), along with a good safety index (CC<sub>50</sub>>64  $\mu$ g/mL). Furthermore, derivative **222** exhibited low hERG-mediated cardiotoxicity and favourable oral pharmacokinetic properties.

Piperazine rings have been found application in the design of enzyme inhibitors. In this regard, the De Luca research group documented the design of new 4-fluorobenzylpiperazine derivatives as tyrosinase inhibitors.<sup>121-125</sup> Tyrosinase is a copper containing enzyme involved in the synthesis of melanin pigments and its inhibition is exploited for the treatment of hyperpigmentation-related disorders.<sup>126</sup> The authors identified the 4-fluorobenzylpiperazine **223** as novel hit compound with an IC<sub>50</sub> value of 85.80  $\mu$ M (Figure 7).<sup>121</sup> Structural optimizations led to two new potent inhibitors, **224** and **225**, able to block tyrosinase activity with IC<sub>50</sub> values equal to 0.96  $\mu$ M and 0.18  $\mu$ M, respectively (Figure 7) proving to be more effective than kojic acid used as reference (IC<sub>50</sub>=17.76  $\mu$ M). Both compounds displayed a competitive mode of action and were able to reduce melanin content in  $\alpha$ -MSH-stimulated B16F10 cells.<sup>123,124</sup>

Liu *et al.* reported the discovery of nonpeptidic piperazine derivatives as potential therapeutic agents for the treatment of SARS-CoV-2 infections.<sup>127</sup> These derivatives covalently target the SARS-CoV-2 Main protease (M<sup>pro</sup>), a cysteine protease which plays a key role in the virus replication and transcription. The most potent compound **226** (Figure 7) inhibited M<sup>pro</sup> with an IC<sub>50</sub> value of 0.18  $\mu$ M exerting good antiviral activity against SARS-CoV-2 in Vero E6 cells (EC<sub>50</sub>=2.64  $\mu$ M) comparable to that of the reference remdesivir (EC<sub>50</sub>=2.27  $\mu$ M). Mass spectrometry along with crystallographic studies supported the covalent binding of **226** to the catalytic cysteine of M<sup>pro</sup> active site. Interestingly, compound **226** exhibited a good selectivity profile towards SARS-CoV-2 M<sup>pro</sup> with respect to other human cysteine proteases.

Du and co-workers reported the anti-inflammatory and neuroprotective activities of novel piperazine-pyrimidine derivatives for the cure of ischemic stroke.<sup>128</sup> Among the synthesized molecules, compound **227**, see Figure 7, exhibited a significant cytoprotective effect against the damages induced by oxygen-glucose deprivation/reoxygenation (ODG/R) in BV2 cells. Moreover, **227** was able to reduce the release of inflammatory mediators such as tumor necrosis factor- $\alpha$  (TNF- $\alpha$ ), interleukin-1 $\beta$  (IL-1 $\beta$ ), IL-6, nitric oxide and prostaglandin E<sub>2</sub> from lipopolysaccharide (LPS) induced BV2 cells. In addition, the reduction of TNF- $\alpha$  and IL-1 $\beta$  was also observed *in vivo* from LPS-induced mouse brain neuroinflammation model. *In vitro* tests revealed that **227** was a potent inhibitor of cyclooxygenase-2 (COX-2) and 5-lipoxygenase (5-LOX) showing IC<sub>50</sub> values of 92.54 nM and 41.86 nM, respectively. Interestingly, compound **227** exerted significant neuroprotective properties in middle cerebral artery occlusion rats decreasing their infarct volumes and neurological deficit scores.

Onnis and collaborators described the inhibitory activity of a novel series of piperazine-containing sulfonamide derivatives targeting human carbonic anhydrase (hCA) enzyme.<sup>129</sup> The latter is a zinc-containing enzyme catalysing the reversible hydration of carbon dioxide to bicarbonate and proton. Specifically, hCAIX and hCAXII isoforms are implicated in tumorigenesis and are, therefore, considered as target for cancer therapy.<sup>130</sup> Among the tested compounds, derivative **228** (Figure 7) showed the best inhibitory profile with a higher affinity towards the tumor-associated isoforms hCAIX ( $K_i=8.3$  nM) and hCAXII ( $K_i=2.7$  nM) with respect to the ubiquitous isoforms hCAI ( $K_i=47.3$  nM) and hCAII ( $K_i=36.5$  nM). In addition, inhibitor **228** proved to be more potent on the tumor-associated isoforms than the reference acetazolamide (hCA IX,  $K_i=25.8$  nM, hCA XII,  $K_i=5.7$  nM).<sup>129</sup>

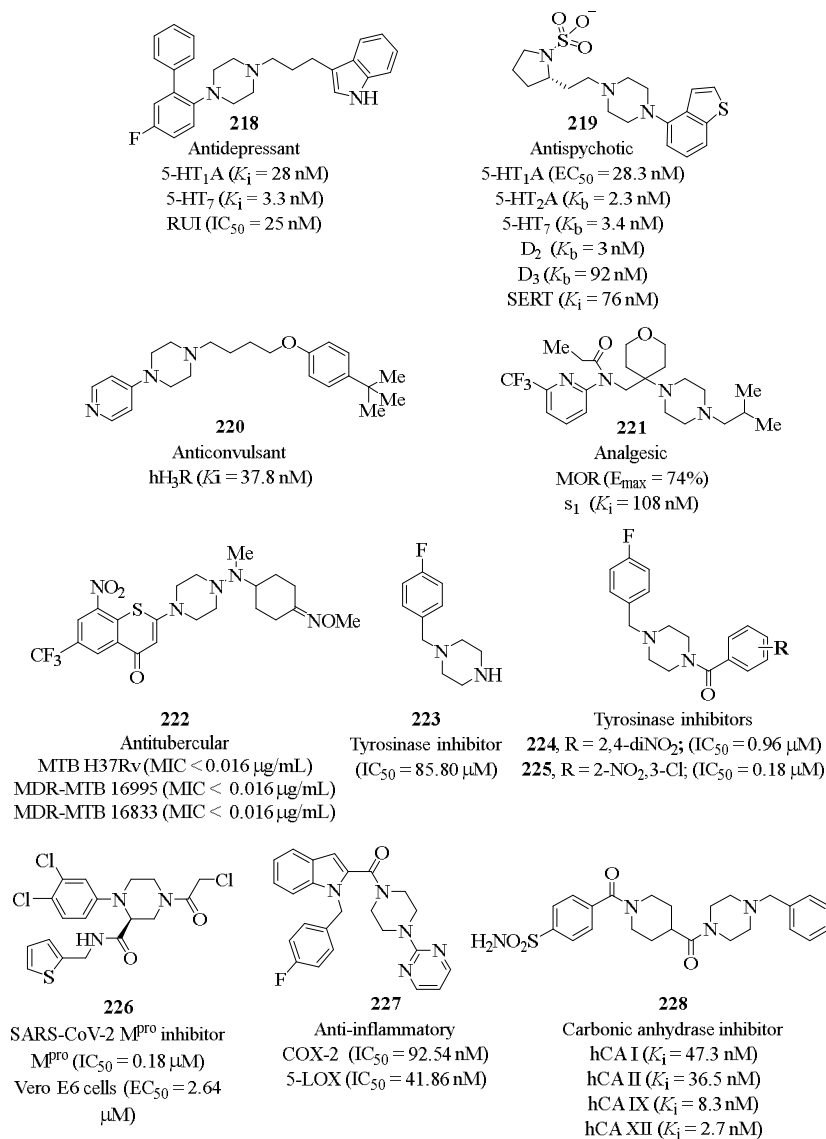


**Figure 7.** Biological activities of piperazine containing derivatives.

## 5. Conclusion

Five- and six-membered heterocycles are among the most common compounds in organic chemistry. They possess a cyclic structure, with one or more fused rings, bearing at least one heteroatom (*e.g.* nitrogen, oxygen, sulfur). Among them, nitrogen-containing heterocycles have a wide application in medicinal chemistry. Due to their unique features, aziridine-, triazole-, and piperazine moieties are incorporated in several drugs enabling to modulate their target affinity and physicochemical properties.

For these reasons, the synthetic approaches and biological applications are manifold and the interest in these compounds will prevail, leading to more research on these structural motifs.

## Acknowledgements

The authors thank the University of Turin and the University of Vienna for financial support. The authors acknowledge support from Project CH4.0 under the MUR (Italian Ministry for the University) program “Dipartimenti di Eccellenza 2023–2027” (CUP: D13C22003520001).

## References

1. Arora, P.; Arora, V.; Lamba, H.; Wadhwa, D. *Int. J. Pharm. Sci. Res.* **2012**, *3*, 2947.
2. Dank, C.; Ielo, L. *Org. Biomol. Chem.* **2023**, *21*, 4553-4573.
3. He, J.; Ling, J.; Chiu, P. *Chem. Rev.* **2014**, *114*, 8037-8128.
4. Zélcans, G.; Gervay-Hague, J.; Maulie, I., Ethylene Sulfide. In *Encyclopedia of Reagents for Organic Synthesis*.
5. Kottke, R. *Kirk-Othmer Encyclopedia of Chemical Technology* **2000**.
6. Mishra, R.; Jha, K.; Kumar, S.; Tomer, I. *Der Pharma Chem.* **2011**, *3*, 38-54.
7. Baltazzi, E.; Krimen, L. I. *Chem. Rev.* **1963**, *63*, 511-556.
8. Kütükgüzel, Ş. G.; Şenkardeş, S. *Eur. J. Med. Chem.* **2015**, *97*, 786-815.
9. Bhatnagar, A.; Sharma, P.; Kumar, N. *Int. J. Pharm. Tech. Res.* **2011**, *3*, 268-282.
10. Citarella, A.; Ielo, L.; Stagno, C.; Cristani, M.; Muscarà, C.; Pace, V.; Micale, N. *Org. Biomol. Chem.* **2022**, *20*, 8293-8304.
11. Altaf, A. A.; Shahzad, A.; Gul, Z.; Rasool, N.; Badshah, A.; Lal, B.; Khan, E. *J. Drug Des. Med. Chem.* **2015**, *1*, 1-11.
12. Schoeggli Toledano, A.; Bitai, J.; Covini, D.; Karolyi-Oezguer, J.; Dank, C.; Berger, H.; Gollner, A. *Org. Lett.* **2024**, *26*, 1229-1232.
13. Citarella, A.; Vittorio, S.; Dank, C.; Ielo, L. *Front. Chem.* **2024**, *12*, 1362992.
14. Khanam, H. *Eur. J. Med. Chem.* **2015**, *97*, 483-504.
15. Legraverend, M.; Grierson, D. S. *Bioorg. Med. Chem.* **2006**, *14*, 3987-4006.
16. Ram, V. J.; Sethi, A.; Nath, M.; Pratap, R., *The chemistry of heterocycles: Chemistry of six to eight membered N, O, S, P and Se heterocycles*. Elsevier: 2019.
17. Wu, Y.-J., Chapter 1 - Heterocycles and Medicine: A Survey of the Heterocyclic Drugs Approved by the U.S. FDA from 2000 to Present. In *Progress in Heterocyclic Chemistry*, Gribble, G. W.; Joule, J. A., Eds. Elsevier: 2012; Vol. 24, pp 1-53.
18. Qadir, T.; Amin, A.; Sarkar, D.; Sharma, K. P. *Curr. Org. Chem.* **2021**, *25*, 1868-1893.
19. Sahu, J. K.; Ganguly, S.; Kaushik, A. *Chin. J. Nat. Med.* **2013**, *11*, 456-465.
20. Gettys, K. E.; Ye, Z.; Dai, M. *Synthesis* **2017**, *49*, 2589-2604.
21. Durand, C.; Szostak, M. *Organics* **2021**, *2*, 337-347.
22. Sweeney, J. B. *Chem. Soc. Rev.* **2002**, *31*, 247-258.
23. Singh, G. S.; D'Hooghe, M.; De Kimpe, N. *Chem. Rev.* **2007**, *107*, 2080-2135.
24. Wang, H.; Yang, J. C.; Buchwald, S. L. *J. Am. Chem. Soc.* **2017**, *139*, 8428-8431.
25. Chen, S.; Yao, Y.; Yang, W.; Lin, Q.; Wang, L.; Li, H.; Chen, D.; Tan, Y.; Yang, D. *J. Org. Chem.* **2019**, *84*, 11863-11872.
26. Chavan, S. P.; Kawale, S. A.; Gonnade, R. G. *Eur. J. Org. Chem.* **2022**, *2022*, e202200384.
27. Chavan, S. P.; Kadam, A. L.; Shinde, S. S.; Gonnade, R. G. *Chem. Asian J.* **2020**, *15*, 415-424.
28. Prieschl, M.; Cantillo, D.; Kappe, C. O. *J. Flow. Chem.* **2021**, *11*, 117-125.
29. Tan, H.; Samanta, S.; Maity, A.; Roychowdhury, P.; Powers, D. C. *Nat. Commun.* **2022**, *13*, 3341-3349.



30. Rodríguez, M. R.; M Rodríguez, A.; López-Resano, S.; Pericàs, M. A.; Díaz-Requejo, M. M.; Maseras, F.; Pérez, P. J. *ACS Catal.* **2023**, *13*, 706-713.
31. Baris, N.; Dračinský, M.; Tarábek, J.; Filgas, J.; Slaviček, P.; Ludvíková, L.; Boháčová, S.; Slanina, T.; Klepetářová, B.; Beier, P. *Angew. Chem. Int. Ed.* **2024**, *63*, e202315162.
32. Pan, J.; Wu, J.-H.; Zhang, H.; Ren, X.; Tan, J.-P.; Zhu, L.; Zhang, H.-S.; Jiang, C.; Wang, T. *Angew. Chem. Int. Ed.* **2019**, *58*, 7425-7430.
33. Ielo, L.; Touqeer, S.; Roller, A.; Langer, T.; Holzer, W.; Pace, V. *Angew. Chem. Int. Ed.* **2019**, *58*, 2479-2484.
34. Monticelli, S.; Colella, M.; Pillari, V.; Tota, A.; Langer, T.; Holzer, W.; Degennaro, L.; Luisi, R.; Pace, V. *Org. Lett.* **2019**, *21*, 584-588.
35. Wölfl, B.; Winter, N.; Li, J.; Noble, A.; Aggarwal, V. K. *Angew. Chem. Int. Ed.* **2023**, *62*, e202217064.
36. Banuprakash Goud, S.; Lal Dhakar, R.; Samanta, S. *Chem. Asian J.* **2024**, *19*, e202300904.
37. Thi, H. D.; Thuy, G. L. N.; Catak, S.; Van Speybroeck, V.; Van Nguyen, T.; D'hooghe, M. *Synthesis* **2018**, *50*, 1439-1456.
38. Wu, K.; Zhou, C.-Y.; Che, C.-M. *Org. Lett.* **2019**, *21*, 85-89.
39. Andresini, M.; Degennaro, L.; Luisi, R. *Beilstein J. Org. Chem.* **2021**, *17*, 203-209.
40. Zhao, Z. Y.; Cui, M.; Irran, E.; Oestreich, M. *Angew. Chem. Int. Ed.* **2023**, *62*, e202215032.
41. S Singh, G. *Mini Rev. Med. Chem.* **2016**, *16*, 892-904.
42. Karati, D.; Mahadik, K. R.; Trivedi, P.; Kumar, D. *Anti-Cancer Agents Med. Chem.* **2022**, *22*, 1478-1495.
43. Buback, V.; Mladenovic, M.; Engels, B.; Schirmeister, T. *J. Phys. Chem. B* **2009**, *113*, 5282-5289.
44. Rowland, R. J.; Chen, Y.; Breen, I.; Wu, L.; Offen, W. A.; Beenakker, T. J.; Su, Q.; van den Nieuwendijk, A. M.; Aerts, J. M.; Artola, M. *Chem. Eur. J.* **2021**, *27*, 16377-16388.
45. Sarojini, P.; Jeyachandran, M.; Sriram, D.; Ranganathan, P.; Gandhimathi, S. *J. Mol. Struct.* **2021**, *1233*, 130038.
46. Cavalli, A.; Bolognesi, M. L. *J. Med. Chem.* **2009**, *52*, 7339-7359.
47. Sert, M.; Işilar, Ö.; Yaglioglu, A. S.; Bulut, A. *Carbohydr. Res.* **2021**, *509*, 108430.
48. Zelencova-Gopejenko, D.; Andrianov, V.; Domracheva, I.; Kanepe-Lapsa, I.; Milczarek, M.; Stojak, M.; Przyborowski, K.; Fedak, F. A.; Walczak, M.; Kramkowski, K.; Wietrzyk, J.; Chlopicki, S.; Kalvins, I. *J. Enzyme Inhib. Med. Chem.* **2023**, *38*, 2158187.
49. Ielo, L.; Patamia, V.; Citarella, A.; Efferth, T.; Shahhamzehei, N.; Schirmeister, T.; Stagno, C.; Langer, T.; Rescifina, A.; Micala, N. *Int. J. Mol. Sci.* **2022**, *23*, 12363.
50. Ielo, L.; Patamia, V.; Citarella, A.; Schirmeister, T.; Stagno, C.; Rescifina, A.; Micala, N.; Pace, V. *Arch. Pharm.* **2023**, *356*, 2300174.
51. Chaudhari, P. J.; Bari, S. B.; Surana, S. J.; Shirkhedkar, A. A.; Bonde, C. G.; Khadse, S. C.; Ugale, V. G.; Nagar, A. A.; Cheke, R. S. *ACS Omega* **2022**, *7*, 17270-17294.
52. Burgos-Morón, E.; Pastor, N.; Orta, M. L.; Jiménez-Alonso, J. J.; Palo-Nieto, C.; Vega-Holm, M.; Vega-Pérez, J. M.; Iglesias-Guerra, F.; Mateos, S.; López-Lázaro, M.; Calderón-Montaño, J. M. *Biomedicines* **2021**, *10*, 41.
53. Giovine, A.; Muraglia, M.; Florio, M. A.; Rosato, A.; Corbo, F.; Franchini, C.; Musio, B.; Degennaro, L.; Luisi, R. *Molecules* **2014**, *19*, 11505-11519.
54. Caridha, D.; Sciotti, R. J.; Sousa, J.; Vesely, B.; Teshome, T.; Bonkougou, G.; Vuong, C.; Leed, S.; Khraiweh, M.; Penn, E.; Kreishman-Deitrick, M.; Lee, P.; Pybus, B.; Lazo, J. S.; Sharlow, E. R. *ACS Infect. Dis.* **2021**, *7*, 506-517.
55. Matin, M. M.; Matin, P.; Rahman, M. R.; Ben Hadda, T.; Almalki, F. A.; Mahmud, S.; Ghoneim, M. M.; Alruwaily, M.; Alshehri, S. *Front. Mol. Biosci.* **2022**, *9*, 864286.
56. Guan, Q.; Xing, S.; Wang, L.; Zhu, J.; Guo, C.; Xu, C.; Zhao, Q.; Wu, Y.; Chen, Y.; Sun, H. *J. Med. Chem.* **2024**, *67*, 7788-7824.
57. Agalave, S. G.; Maujan, S. R.; Pore, V. S. *Chem. Asian J.* **2011**, *6*, 2696-2718.
58. Rostovtsev, V. V.; Green, L. G.; Fokin, V. V.; Sharpless, K. B. *Angew. Chem. Int. Ed.* **2002**, *41*, 2596-2599.
59. Chen, R.; Zeng, L.; Lai, Z.; Cui, S. *Adv. Synth. Cat.* **2019**, *361*, 989-994.

60. Giel, M. C.; Smedley, C. J.; Mackie, E. R. R.; Guo, T.; Dong, J.; Soares da Costa, T. P.; Moses, J. E. *Angew. Chem. Int. Ed.* **2020**, *59*, 1181-1186.
61. Liu, E. C.; Topczewski, J. J. *J. Am. Chem. Soc.* **2021**, *143*, 5308-5313.
62. Guo, W. T.; Zhu, B. H.; Chen, Y.; Yang, J.; Qian, P. C.; Deng, C.; Ye, L. W.; Li, L. *J. Am. Chem. Soc.* **2022**, *144*, 6981-6991.
63. Zhang, X. P.; Yang, Wang, Haibo; Liang, Chong; Ma, Xiaofeng; Jiao, Wei; Shao, Huawu. *Adv. Synth. Cat.* **2021**, *363*, 459-463.
64. Yang, H.; Xu, T.-H.; Lu, S.-N.; Chen, Z.; Wu, X.-F. *Org. Chem. Front.* **2021**, *8*, 3440-3445.
65. Sai Allaka, B.; Basavoju, S.; Rama Krishna, G. *Adv. Synth. Cat.* **2021**, *363*, 3560-3565.
66. Li, H.; Wu, X.; Hao, W.; Li, H.; Zhao, Y.; Wang, Y.; Lian, P.; Zheng, Y.; Bao, X.; Wan, X. *Org. Lett.* **2018**, *20*, 5224-5227.
67. Tian, Y.-T.; Zhang, F.-G.; Nie, J.; Cheung, C. W.; Ma, J.-A. *Adv. Synth. Cat.* **2021**, *363*, 227-233.
68. Guru, M. M.; De, S.; Dutta, S.; Koley, D.; Maji, B. *Chem. Sci.* **2019**, *10*, 7964-7974.
69. Matsuzaki, H.; Takeda, N.; Yasui, M.; Okazaki, M.; Suzuki, S.; Ueda, M. *Chem. Commun.* **2021**, *57*, 12187-12190.
70. Zhang, C.; Liang, Z.; Jia, X.; Wang, M.; Zhang, G.; Hu, M. L. *Chem. Commun.* **2020**, *56*, 14215-14218.
71. Lu, S.-N.; Yang, H.; Zhang, J.; Chen, Z.; Wu, X.-F. *Adv. Synth. Cat.* **2021**, *363*, 4982-4987.
72. Guo, W.; Liu, G.; Deng, L.; Mei, W.; Zou, X.; Zhong, Y.; Zhuo, X.; Fan, X.; Zheng, L. *J. Org. Chem.* **2021**, *86*, 17986-18003.
73. Monk, B. C.; Sagatova, A. A.; Hosseini, P.; Ruma, Y. N.; Wilson, R. K.; Keniya, M. V. *Biochim. Biophys. Acta Proteins Proteom.* **2020**, *1868*, 140206.
74. De Petris, A.; Crestoni, M. E.; Pirolli, A.; Rovira, C.; Iglesias-Fernández, J.; Chiavarino, B.; Ragno, R.; Fornarini, S. *Polyhedron* **2015**, *90*, 245-251.
75. Fisher, M. C.; Alastruey-Izquierdo, A.; Berman, J.; Bicanic, T.; Bignell, E. M.; Bowyer, P.; Bromley, M.; Bruggemann, R.; Garber, G.; Cornely, O. A.; Gurr, S. J.; Harrison, T. S.; Kuijper, E.; Rhodes, J.; Sheppard, D. C.; Warris, A.; White, P. L.; Xu, J.; Zwaan, B.; Verweij, P. E. *Nat. Rev. Microbiol.* **2022**, *20*, 557-571.
76. Xie, F.; Hao, Y.; Li, L.; Wang, R.; Bao, J.; Chi, X.; Monk, B. C.; Wang, T.; Yu, S.; Jin, Y.; Zhang, D.; Ni, T.; Yan, L. *Eur. J. Med. Chem.* **2023**, *257*, 115506.
77. Yan, X.; Lv, Z.; Wen, J.; Zhao, S.; Xu, Z. *Eur. J. Med. Chem.* **2018**, *143*, 899-904.
78. Singh, A.; Singh, K.; Kaur, K.; Sharma, A.; Mohana, P.; Prajapati, J.; Kaur, U.; Goswami, D.; Arora, S.; Chadha, R.; Bedi, P. M. S. *Eur. J. Med. Chem.* **2024**, *263*, 115948.
79. Ye, G. J.; Lan, T.; Huang, Z. X.; Cheng, X. N.; Cai, C. Y.; Ding, S. M.; Xie, M. L.; Wang, B. *Eur. J. Med. Chem.* **2019**, *177*, 362-373.
80. Vittorio, S.; Adornato, I.; Gitto, R.; Pena-Diaz, S.; Ventura, S.; De Luca, L. *J. Enzyme Inhib. Med. Chem.* **2020**, *35*, 1727-1735.
81. De Luca, L.; Vittorio, S.; Pena-Diaz, S.; Pitasi, G.; Fornt-Sune, M.; Bucolo, F.; Ventura, S.; Gitto, R. *Int. J. Mol. Sci.* **2022**, *23*, 14844.
82. Gitto, R.; Vittorio, S.; Bucolo, F.; Pena-Diaz, S.; Siracusa, R.; Cuzzocrea, S.; Ventura, S.; Di Paola, R.; De Luca, L. *ACS Chem. Neurosci.* **2022**, *13*, 581-586.
83. Kumar, A.; Lal, K.; Kumar, V.; Murtaza, M.; Jaglan, S.; Paul, A. K.; Yadav, S.; Kumari, K. *Bioorg. Chem.* **2023**, *133*, 106388.
84. Lane, T.; Makarov, V.; Nelson, J. A. E.; Meeker, R. B.; Sanna, G.; Riabova, O.; Kazakova, E.; Monakhova, N.; Tsedilin, A.; Urbina, F.; Jones, T.; Suchy, A.; Ekins, S. *J. Med. Chem.* **2023**, *66*, 6193-6217.
85. Yevale, D.; Teraiya, N.; Lalwani, T.; Dalasaniya, M.; Kapadiya, K.; Ameta, R. K.; Sangani, C. B.; Duan, Y. T. *Bioorg. Chem.* **2024**, *147*, 107323.
86. Vittorio, S.; Gitto, R.; Adornato, I.; Russo, E.; De Luca, L. *Molecules* **2021**, *26*, 1103.
87. Vitaku, E.; Smith, D. T.; Njardarson, J. T. *J. Med. Chem.* **2014**, *57*, 10257-10274.
88. Walker, M. A. *Expert Opin. Drug Dis.* **2014**, *9*, 1421-1433.
89. Sánchez-Roselló, M.; Delgado, O.; Mateu, N.; Trabanco, A. A.; Van Gool, M.; Fustero, S. *J. Org. Chem.* **2014**, *79*, 5887-5894.

90. Ruppert, I.; Schlich, K.; Volbach, W. *Tetrahedron Lett.* **1984**, *25*, 2195-2198.
91. Prakash, G. S.; Krishnamurti, R.; Olah, G. A. *J. Am. Chem. Soc.* **1989**, *111*, 393-395.
92. Robak, M. T.; Herbage, M. A.; Ellman, J. A. *Chem. Rev.* **2010**, *110*, 3600-3740.
93. Cushman, M.; Castagnoli Jr, N. *J. Org. Chem.* **1972**, *37*, 1268-1271.
94. Dar'ın, D.; Bakulina, O.; Chizhova, M.; Krasavin, M. *Org. Lett.* **2015**, *17*, 3930-3933.
95. Yar, M.; McGarrigle, E. M.; Aggarwal, V. K. *Angew. Chem. Int. Ed.* **2008**, *47*, 3784-3786.
96. Bagnoli, L.; Scarponi, C.; Rossi, M. G.; Testaferri, L.; Tiecco, M. *Chem. Eur. J.* **2011**, *17*, 993-999.
97. McNally, A.; Prier, C. K.; MacMillan, D. W. *Science* **2011**, *334*, 1114-1117.
98. Noble, A.; MacMillan, D. W. *J. Am. Chem. Soc.* **2014**, *136*, 11602-11605.
99. Prier, C. K.; MacMillan, D. W. *Chem. Sci.* **2014**, *5*, 4173-4178.
100. McManus, J. B.; Onuska, N. P.; Nicewicz, D. A. *J. Am. Chem. Soc.* **2018**, *140*, 9056-9060.
101. McManus, J. B.; Onuska, N. P.; Jeffreys, M. S.; Goodwin, N. C.; Nicewicz, D. A. *Org. Lett.* **2020**, *22*, 679-683.
102. Vo, C. V. T.; Mikutis, G.; Bode, J. W. *Angew. Chem. Int. Ed.* **2013**, *52*, 1705-1708.
103. Vo, C.-V. T.; Luescher, M. U.; Bode, J. W. *Nat. Chem.* **2014**, *6*, 310-314.
104. Luescher, M. U.; Vo, C.-V. T.; Bode, J. W. *Org. Lett.* **2014**, *16*, 1236-1239.
105. Luescher, M. U.; Bode, J. W. *Angew. Chem. Int. Ed.* **2015**, *54*, 10884-10888.
106. Siau, W.-Y.; Bode, J. W. *J. Am. Chem. Soc.* **2014**, *136*, 17726-17729.
107. Hsieh, S.-Y.; Bode, J. W. *Org. Lett.* **2016**, *18*, 2098-2101.
108. Gueret, R.; Pelinski, L.; Bousquet, T.; Sauthier, M.; Ferey, V.; Bigot, A. *Org. Lett.* **2020**, *22*, 5157-5162.
109. Trinchera, P.; Musio, B.; Degennaro, L.; Moliterni, A.; Falcicchio, A.; Luisi, R. *Org. Biomol. Chem.* **2012**, *10*, 1962-1965.
110. Suárez-Pantiga, S.; Colas, K.; Johansson, M. J.; Mendoza, A. *Angew. Chem. Int. Ed.* **2015**, *54*, 14094-14098.
111. Yavari, I.; Bayat, M. J.; Ghazanfarpour-Darjani, M. *Tetrahedron Lett.* **2014**, *55*, 5595-5596.
112. Dong, H.-R.; Chen, Z.-B.; Li, R.-S.; Dong, H.-S.; Xie, Z.-X. *RSC Adv.* **2015**, *5*, 10768-10772.
113. Ruider, S. A.; Müller, S.; Carreira, E. M. *Angew. Chem. Int. Ed.* **2013**, *52*, 11908-11911.
114. Wang, J.; Liu, X.; Feng, X. *Chem. Rev.* **2011**, *111*, 6947-6983.
115. Gu, Z. S.; Zhou, A. N.; Xiao, Y.; Zhang, Q. W.; Li, J. Q. *Eur. J. Med. Chem.* **2018**, *144*, 701-715.
116. Millan, M. J. *Neurotherapeutics* **2009**, *6*, 53-77.
117. Zajdel, P.; Kos, T.; Marciniec, K.; Satala, G.; Canale, V.; Kaminski, K.; Holuj, M.; Lenda, T.; Koralewski, R.; Bednarski, M.; Nowinski, L.; Wojcikowski, J.; Daniel, W. A.; Nikiforuk, A.; Nalepa, I.; Chmielarczyk, P.; Kusmierczyk, J.; Bojarski, A. J.; Popik, P. *Eur. J. Med. Chem.* **2018**, *145*, 790-804.
118. Szczepanska, K.; Karcz, T.; Mogilski, S.; Siwek, A.; Kuder, K. J.; Latacz, G.; Kubacka, M.; Hagenow, S.; Lubelska, A.; Olejarz, A.; Kotanska, M.; Sadek, B.; Stark, H.; Kiec-Kononowicz, K. *Eur. J. Med. Chem.* **2018**, *152*, 223-234.
119. Garcia, M.; Llorente, V.; Garriga, L.; Christmann, U.; Rodriguez-Esrich, S.; Virgili, M.; Fernandez, B.; Bordas, M.; Ayet, E.; Burgueno, J.; Pujol, M.; Dordal, A.; Portillo-Salido, E.; Gris, G.; Vela, J. M.; Almansa, C. *J. Med. Chem.* **2021**, *64*, 10139-10154.
120. Wang, A.; Xu, S.; Chai, Y.; Xia, G.; Wang, B.; Lv, K.; Ma, C.; Wang, D.; Wang, A.; Qin, X.; Liu, M.; Lu, Y. *Eur. J. Med. Chem.* **2021**, *218*, 113398.
121. De Luca, L.; Germano, M. P.; Fais, A.; Pintus, F.; Buemi, M. R.; Vittorio, S.; Mirabile, S.; Rapisarda, A.; Gitto, R. *Bioorg. Med. Chem.* **2020**, *28*, 115497.
122. Ferro, S.; Deri, B.; Germano, M. P.; Gitto, R.; Ielo, L.; Buemi, M. R.; Certo, G.; Vittorio, S.; Rapisarda, A.; Pazy, Y.; Fishman, A.; De Luca, L. *J. Med. Chem.* **2018**, *61*, 3908-3917.
123. Ielo, L.; Deri, B.; Germano, M. P.; Vittorio, S.; Mirabile, S.; Gitto, R.; Rapisarda, A.; Ronsisvalle, S.; Floris, S.; Pazy, Y.; Fais, A.; Fishman, A.; De Luca, L. *Eur. J. Med. Chem.* **2019**, *178*, 380-389.
124. Mirabile, S.; Vittorio, S.; Paola Germano, M.; Adornato, I.; Ielo, L.; Rapisarda, A.; Gitto, R.; Pintus, F.; Fais, A.; De Luca, L. *ChemMedChem* **2021**, *16*, 3083-3093.
125. Vittorio, S.; Ielo, L.; Mirabile, S.; Gitto, R.; Fais, A.; Floris, S.; Rapisarda, A.; Germano, M. P.; De Luca, L. *ChemMedChem* **2020**, *15*, 1757-1764.
126. Vittorio, S.; Dank, C.; Ielo, L. *Int. J. Mol. Sci.* **2023**, *24*, 9097.

127. Gao, S.; Song, L.; Claff, T.; Woodson, M.; Sylvester, K.; Jing, L.; Weisse, R. H.; Cheng, Y.; Strater, N.; Schakel, L.; Gutschow, M.; Ye, B.; Yang, M.; Zhang, T.; Kang, D.; Toth, K.; Tavis, J.; Tollefson, A. E.; Muller, C. E.; Zhan, P.; Liu, X. *J. Med. Chem.* **2022**, *65*, 16902-16917.
128. Wang, H.; Cui, E.; Li, J.; Ma, X.; Jiang, X.; Du, S.; Qian, S.; Du, L. *Eur. J. Med. Chem.* **2022**, *241*, 114597.
129. Moi, D.; Vittorio, S.; Angeli, A.; Supuran, C. T.; Onnis, V. *ACS Med. Chem. Lett.* **2024**, *15*, 470-477.
130. Moi, D.; Vittorio, S.; Angeli, A.; Balboni, G.; Supuran, C. T.; Onnis, V. *Molecules* **2022**, *28*, 91.